The Journal of Neuroscience, October 1991, 11(10): 3079–3095

Voltage-sensitive Potassium Channels in *Drosophila* Photoreceptors

R. C. Hardie

Cambridge University, Department of Zoology, Cambridge CB2 3EJ, United Kingdom

A preparation of dissociated *Drosophila* ommatidia is described that allows single-channel and whole-cell patch-clamp analysis of currents in identified sensory neurons. Three distinct classes of voltage-sensitive potassium conductances are characterized; all were detected in distal parts of ommatidia from *sevenless* mutants and hence in one cell class (R1–6 photoreceptors). Rapidly inactivating A-channels (I_A), coded by the *Shaker* gene, were isolated in multichannel patches from adult flies. While showing similar kinetics to muscle A-channels, they differ from previously characterized wild-type *Shaker* channels in having a much more negative voltage operating range, being half-inactivated at ≈ −70 mV. Two delayed rectifier conductances were characterized in whole-cell recordings from pupal photoreceptors. The most commonly encountered class (I_{Ks}) is similar to previously reported delayed rectifier conductances in *Drosophila*. It inactivates slowly (time constant, ≈500 msec) and is half-inactivated at ≈ −40 mV. A more rapidly inactivating delayed rectifier (I_{Kf}) was detected in ≈30% of cells; it is half-inactivated at ≈ −80 mV. Both I_{Ks} and I_{Kf} are blocked by 100 μM quinidine. Neither are greatly affected by 4-aminopyridine, which blocks I_A at 1–5 mM. None of the three conductances was calcium dependent, nor were they obviously affected by the *eag* mutation, which affects K channels in muscle. The developmental profile of the channels is the inverse of that described in muscle. Both I_{Ks} and I_{Kf} are present at the earliest pupal stages examined (≈60 hr), but I_A was only first detected at ≈76 hr. This novel preparation will not only facilitate the molecular and genetic analysis of native ion channels in identified cells but, because of our extensive knowledge of photoreceptor function, will allow a critical functional evaluation of channel properties *in situ*.

Potassium channels are generally considered to represent the most diverse of the ion channel families (reviews: Hille, 1984; Rudy, 1988). It is now possible to explore both the biophysics and the molecular biology of specific potassium channels in a number of *in vivo* and *in vitro* systems; however, the advantages of the molecular genetic approach have made *Drosophila* one of the most favored preparations (reviews: Salkoff, 1983; Ganetzky and Wu, 1985; Salkoff and Tanouye, 1986; Papazian et al., 1988). A conspicuous success has been the cloning and expression of the first K channel gene, *Shaker* (Baumann et al., 1987; Kamb et al., 1987; Papazian et al., 1987; Tempel et al., 1987), which has been shown to be responsible for a rapidly inactivating A-current in muscle (Salkoff and Wyman, 1981b; Wu and Haugland, 1985). With the cloning of the gene came the discovery that the *Shaker* locus potentially coded for a variety of K channels by mechanisms of alternative splicing (Iverson et al., 1988; Kamb et al., 1988; Pongs et al., 1988; Schwarz et al., 1988; Timpe et al., 1988) and heteromultimeric combinations (Isacoff et al., 1990; McCormack et al., 1990). Subsequently, a number of related genes (*Shal, Shab,* and *Shaw*) were isolated by homology (Butler et al., 1989) and shown in oocyte expression studies to code for yet further potassium channels with a range of functional properties (Wei et al., 1990).

Despite this molecular palette and substantial evidence indicating the presence of *Shaker* gene products in the *Drosophila* nervous system (Tanouye et al., 1981; Wu et al., 1983a; Pongs et al., 1988; Schwarz et al., 1990), little progress has been made in identifying particular molecular species of potassium channels *in situ*. The lack of mutants has thus far hindered the identification of native *Shal, Shab,* and *Shaw* channels, and until recently the only native *Shaker* channel to have been characterized was the A-channel in muscle. While it is possible to patch-clamp dissociated and cultured *Drosophila* neurons, most of the K channels described are apparently not coded by the *Shaker* gene (e.g., Solc and Aldrich, 1988), although Baker and Salkoff (1990) have presented statistical arguments indicating that a subset of CNS cell bodies expresses *Shaker* channels. One reason for the lack of progress may be that, apart from the muscle preparations, previous patch-clamp studies in *Drosophila* have relied upon unidentified neurons extracted from entire brains or ganglia (e.g., Wu et al., 1983b; Byerly and Leung, 1988; Solc and Aldrich, 1988; Baker and Salkoff, 1990). Not surprisingly, therefore, cells exhibit a heterogeneity of conductance mechanisms that hinders a more detailed analysis.

Arguably the most thoroughly studied cell type in *Drosophila* from a molecular genetic point of view are the photoreceptors (reviews: Pak, 1979, 1991; Selinger and Minke, 1988). A number of electrophysiological studies have also been performed on these cells (e.g., Wu and Pak, 1975; Johnson and Pak, 1986), but previous investigations, employing conventional intracellular and extracellular recording techniques, have not allowed the analysis of specific conductance mechanisms. Recently, a preparation of dissociated ommatidia from the *Drosophila* retina has been developed (Hardie et al., 1991), in which the photoreceptors prove amenable to both single-channel and whole-cell recordings. The present article describes three dominant voltage-sensitive potassium conductances found in this preparation. These include a rapidly inactivating A-current, coded

Received Feb. 19, 1991; revised May 2, 1991; accepted May 13, 1991.

This research was supported by grants from the S.E.R.C. and the Royal Society. I thank Prof. O. Pongs (Bochum), Drs. A. Tomlinson and B. Ganetzky for stocks of mutants, Dr. R. Drysdale for discussing unpublished data, and Drs. S. Laughlin, C. Leech, and D. Skingsley for helpful comments on the manuscript.

Correspondence should be addressed to R. C. Hardie, Cambridge University, Department of Zoology, Downing Street, Cambridge CB2 3EJ, United Kingdom.

Copyright © 1991 Society for Neuroscience 0270-6474/91/113079-17$05.00/0

for by the *Shaker* locus (Hardie et al., 1991), and two classes of delayed rectifier–type conductances that differ in their voltage dependency and rate of inactivation. By appropriate procedures, each current can be voltage-clamped in virtually complete isolation. As we already have shown for the case of A-channels coded by the *Shaker* gene (Hardie et al., 1991), the preparation is also suitable for detailed molecular and genetic analysis.

Some of the properties of the *Shaker* A-channels described in this article have been reported in brief previously (Hardie et al., 1991).

Materials and Methods

Fly stocks

The wild-type strain was Oregon R. Two mutations of the *Shaker* locus were used to eliminate the fast A-current: Sh^{KS133}, a mis-sense mutation in the core region of the *Shaker* locus (Lichtinghagen et al., 1990), and Sh^{KS2a}, a chromosomal rearrangement in the *Shaker* region (Schwarz et al., 1988). Neither mutant produces functional A-channels.

Currents were also recorded from *eag* mutants in which both delayed rectifier current and A-currents are affected in larval muscle (Wu et al., 1983a). The allele used was $In(1)sc^{29}$, *wa*; while not previously examined in voltage clamp, the allele involves an inversion with the breakpoint within the *eag* locus and is almost certainly null (Drysdale et al., 1991). To exclude the possibility that any of the currents investigated were restricted to photoreceptors other than R1–6, a number of experiments were performed on *sevenless* flies, which lack photoreceptor class R7 (Harris et al., 1976). The protein-negative allele sev^{d2} was used. Pupal stages were determined according to the criteria of Bainbridge and Bownes (1981).

Preparation

Adult or pupal *Drosophila* ommatidia were prepared as described previously (Hardie et al., 1991). Briefly, retinas were rapidly dissected in normal Ringer's solution, transferred to Ringer's solution supplemented with 10% fetal calf serum (FCS Ringer), and gently triturated with an unsiliconized glass pipette fire polished to a diameter of ≈100–150 μm. During the dissociation procedure, which requires no enzyme treatment, the surrounding pigment cells disintegrate, exposing the photoreceptor membrane that forms giga-seals with a success rate approaching 100%. The procedure also results in the ommatidia breaking off at the basement membrane; thus, the photoreceptors lack their axon terminals. Ommatidia were used immediately or stored in FCS Ringer for several hours at 4°C.

Electrophysiology. Aliquots (≈10 μl) of ommatidia were allowed to settle in a small chamber, the bottom of which is formed by a clean coverslip, on the stage of a Nikon TMS inverted microscope. Recordings were made at (21 ± 1)°C, with patch pipettes pulled from borosilicate glass (fiber filled) with resistances of 3–5 MΩ for whole-cell recordings, or 6–12 MΩ for isolated patches. Junction potentials were nulled just prior to seal formation and corrected according to Fenwick et al. (1982a). Whole-cell recordings and isolated inside-out patches were achieved using standard techniques (Hamill et al., 1981; Hardie, 1989; Hardie et al., 1991).

Signals were amplified using an Axopatch-1B (Axon Instruments) patch-clamp amplifier, filtered via an 8-pole Bessel filter, and either sampled on line or digitized on a PCM video recording system at 20 kHz for later analysis. Data were sampled and analyzed using PCLAMP 5.5 software (Axon Instruments) on an IBM AT computer.

Clamp quality. The A-current was analyzed in multichannel cell-attached or inside-out patches from adult photoreceptors. Seal resistances were typically greater than 10 GΩ, and with appropriate corrections for junction potential, patch voltages should not deviate significantly from nominal values within the bandwidth of the recording (2–5 kHz). On-line leak subtraction was used routinely, presenting scaled, inverted templates below activation threshold (−100 mV) in between each averaging cycle.

In whole-cell recordings, series resistances were judged from the series resistance control of the amplifier and repeatedly monitored during the recording; values were typically in the range 6–25 MΩ. Quantitative whole-cell analysis was only performed on photoreceptors from pupae. With input resistances in the range 100–2000 MΩ and maximum currents usually less than 2 nA, series resistance errors (series resistance × total current flowing) could be kept to acceptable levels (<5 mV) using between 65% and 80% series compensation. Even these small series resistance errors were calculated, and appropriate corrections were applied to all data. Leak subtraction was applied by a variety of means: on line (as above), electronically, off line by subtraction of scaled templates to voltage protocols outside the activation range of any voltage-sensitive currents.

A photoreceptor with an input resistance of 250 MΩ (toward the lower end of measured values), diameter of 5 μm, and length of 80 μm (typical length of a p14 ommatidium) should have a length constant of 627 μm (assuming an internal resistivity of 100 Ω·cm and neglecting external resistivity). This should ensure a reasonable space clamp, and with higher input resistances the situation is even more favorable.

Solutions. Standard Ringer used for the bath in most experiments was composed of (in mM) 195 NaCl, 5 KCl, 1.8 $CaCl_2$, 4 $MgCl_2$, and 10 *N*-Tris-(hydroxymethyl)-methyl-2-amino-ethanesulphonic acid (TES). This solution was also used in the pipette for some inside-out and cell-attached patch recordings, but many measurements were made with a high-K Ringer (50–200 mM KCl, 150–0 mM NaCl; otherwise identical). The intracellular solution for electrodes in most whole-cell recording consisted of (in mM) 200 KCl, 5 EGTA, 4 $MgCl_2$, 2 ATP, 10 TES, and 0.5 mM Ca, resulting in a free-Ca concentration of $\approx 10^{-8}$ M, and 2 mM free Mg (junction potential with respect to normal bath Ringer, −3 mV). A similar solution (but without ATP or EGTA, and no added Ca) was also used for perfusing inside-out patches. The pH of all solutions was buffered to pH 7.15.

Results

Basic electrical properties of dissociated ommatidia

Quantitative analysis of whole-cell currents was performed on pupal photoreceptors from late stage p8 (corresponding to ≈60 hr development at 25°C) to p15 (the final pupal stage, 95–100 hr). Input resistances of these cells varied between 100 and 2500 MΩ. The earlier stages tend to have higher input resistances; however, even p15 photoreceptors often have resistances of at least 500 MΩ. As described in Materials and Methods, membrane resistances of 250 MΩ and above should ensure an adequate space clamp. Resting potentials, corrected for a typical seal resistance of 5–10 GΩ, were relatively low (mean, −37 ± 9 mV; $n = 53$), suggesting the presence of a substantial chloride or nonselective cation leak conductance (recordings were made with chloride symmetrically distributed and under conditions where the light-activated conductance might be expected to be chronically activated). Cell capacitance increases with age from ≈3 pF at stage p8 to ≈30 pF at stage p15. This increase in capacitance is attributable both to an increase in photoreceptor length from ≈20 μm to 100 μm and to the development of the microvilli that probably account for at least 90% of the membrane area in adult photoreceptors (e.g., Hardie, 1985; Johnson and Pak, 1986).

It is also possible to make whole-cell recordings from adult wild-type photoreceptors; however, the relatively low input resistances (between 50 and 100 MΩ) and large currents (several nanoamperes) prevent accurate voltage control. Nevertheless, clamp quality is sufficient to give a good qualitative indication of the voltage-sensitive currents present and confirms the presence of similar conductances in adult flies.

When late stage (p14/15) pupal ommatidia are dissociated and recorded from in dim red light, the photoreceptors typically have deeper resting potentials (−54 ± 5 mV; $n = 20$) that are similar to those recorded in "healthy" photoreceptors *in situ* (Johnson and Pak, 1986; S. B. Laughlin, unpublished observations). The cells also often produce responses to light (Fig. 1*c*), but this light-activated current usually runs down within a few minutes, even when Mg-ATP and GTP are included in the

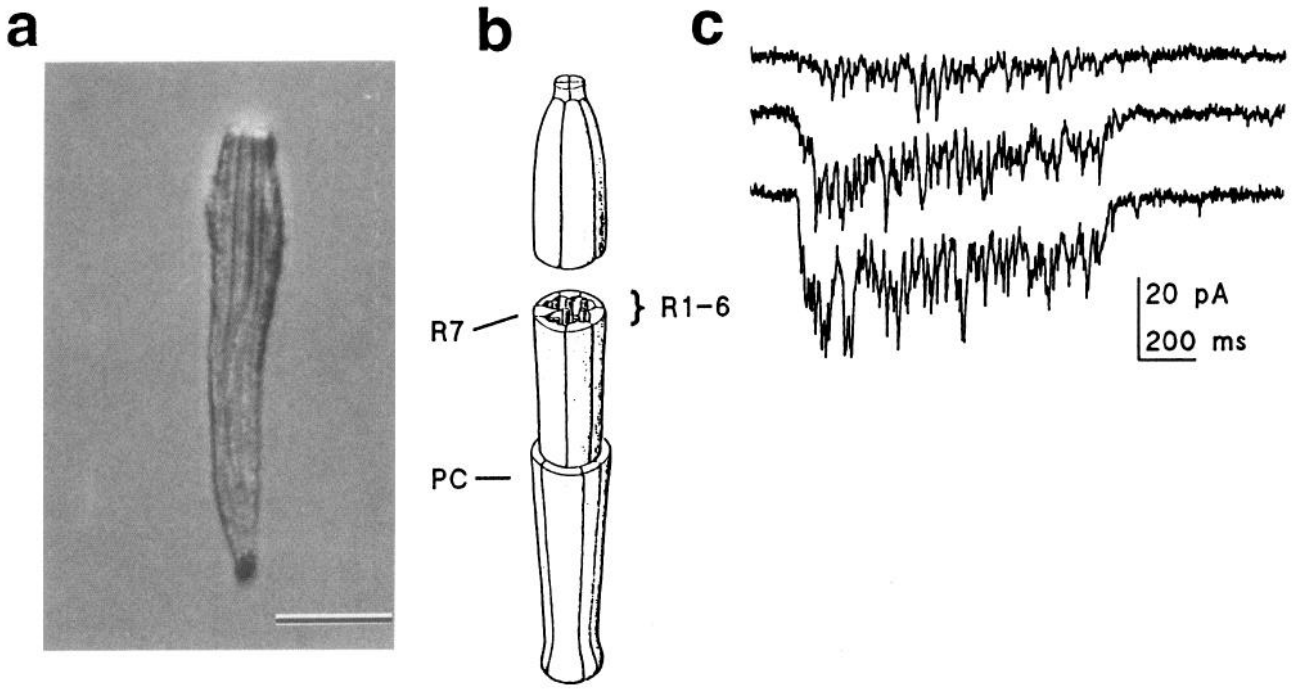

Figure 1. Dissociated ommatidia and whole-cell light responses. *a,* Photomicrograph of dissociated ommatidium from late-stage (p15) pupal compound eye. Indications of the rhabdomeres may be discerned along the length: scale bar, 20 μm. *b,* Cutaway schematic of ommatidial construction consisting of eight photoreceptors (*R1–6, R7,* and *R8*). Visual pigment is contained within the rhabdomeres, light-guiding rod-like structures formed by microvillar extensions within the lumen. The pigment cell sheath (*PC*) is removed by the dissociation procedure allowing access to the photoreceptor membrane; however, notice that only the external surface of each photoreceptor is readily accessible to patch electrodes. *c,* Whole-cell voltage-clamped recording of inward currents induced by light flashes from a green light-emitting diode (three flashes, 1.2 sec, increasing intensities). Most of the noise is due to random absorption of light quanta, although some of the smaller fluctuations may even represent single channels. Holding potential, −60 mV. Wild-type pupal ommatidium (p15). Electrode contained 0.15 mM EGTA, 2 mM Mg-ATP, 0.4 mM GTP, and 195 mM K-gluconate.

whole-cell patch pipette. Since the state of the cells in this respect made no apparent difference to the voltage-sensitive currents (with the exception of the voltage dependence of the delayed rectifier I_{Ks}; see below), the majority of whole-cell recordings were made in normal room light, with 2 mM Mg-ATP but no GTP in the electrode, whereby the phototransduction machinery is apparently completely run down. Under these conditions, the photoreceptor resting potential also decays to zero (without the dialysis afforded by whole-cell recording), as judged by the fact that the apparent voltage dependence of channels is the same in the cell-attached configuration and immediately afterward in inside-out patches. As described previously (Hardie et al., 1991), numerous controls indicate that the properties of the voltage-sensitive potassium currents remain unaltered.

Separation of three outward currents

Whole-cell voltage-clamp recordings of photoreceptors in dissociated ommatidia reveal at least three classes of voltage-dependent outward current (Fig. 2): a rapidly inactivating A-current (I_A) and two slowly inactivating conductances (I_{Ks} and I_{Kf}), which are both referred to here as delayed rectifier–type currents. In addition there is a maintained component to the whole-cell current that may represent yet a further class of noninactivating voltage-sensitive potassium channel.

Several means were used to separate the currents, including the use of mutants, differences in the steady-state inactivation characteristics, pharmacological intervention, and the spatial segregation of channels. From holding potentials more positive than −60 mV, only the most slowly inactivating current (I_{Ks}) is recruited, while the other two can also be observed with prepulses more negative than −70 mV (Fig. 2*a,b*). The most rapidly inactivating current (I_A) is coded for by the *Shaker* locus (Hardie et al., 1991) and is absent in *Shaker* mutants (e.g., Fig. 2*b*). The more rapidly inactivating delayed rectifier (I_{Kf}) was often completely absent, allowing I_{Ks} to be analyzed in isolation (e.g., Fig. 2*c*). I_{Kf} can be isolated by subtraction (e.g., see Figs. 9*b,* 12*b*). In addition, in a minority of recordings, I_{Kf} was the only current obviously present (e.g., see Fig. 12*c*). Both I_{Ks} and I_{Kf} were expressed at the earliest pupal stages examined (late p8 = ≈60 hr) and were investigated in whole-cell recordings from pupae. At later pupal stages (p11–p15) only *Shaker* mutants (Sh^{KS133} and Sh^{K82a}) were used for this purpose.

As described previously (Hardie et al., 1991), A-channels, coded by the *Shaker* gene, were isolated by making use of the finding that, in the majority of cell-attached and inside-out patches, the A-channels are the only voltage-sensitive channels present. Furthermore, the channels are expressed at a conspicuously high density so that reliable macroscopic currents can be synthesized from averaging only a relatively small number (8–32) of voltage protocols. By contrast, other voltage-sensitive channels (possibly corresponding to the delayed rectifier conductance) were observed in less than 5% of patches, and in *Shaker* mutants, the majority of patches contained no voltage-sensitive channels at all. In the dissociated ommatidia, only the external surfaces of the photoreceptors are accessible to the patch electrode (Fig. 1). Since in whole-cell recordings the contributions of the A-current and the two more slowly inactivating currents are approximately equal in magnitude (e.g., Fig. 2*a*),

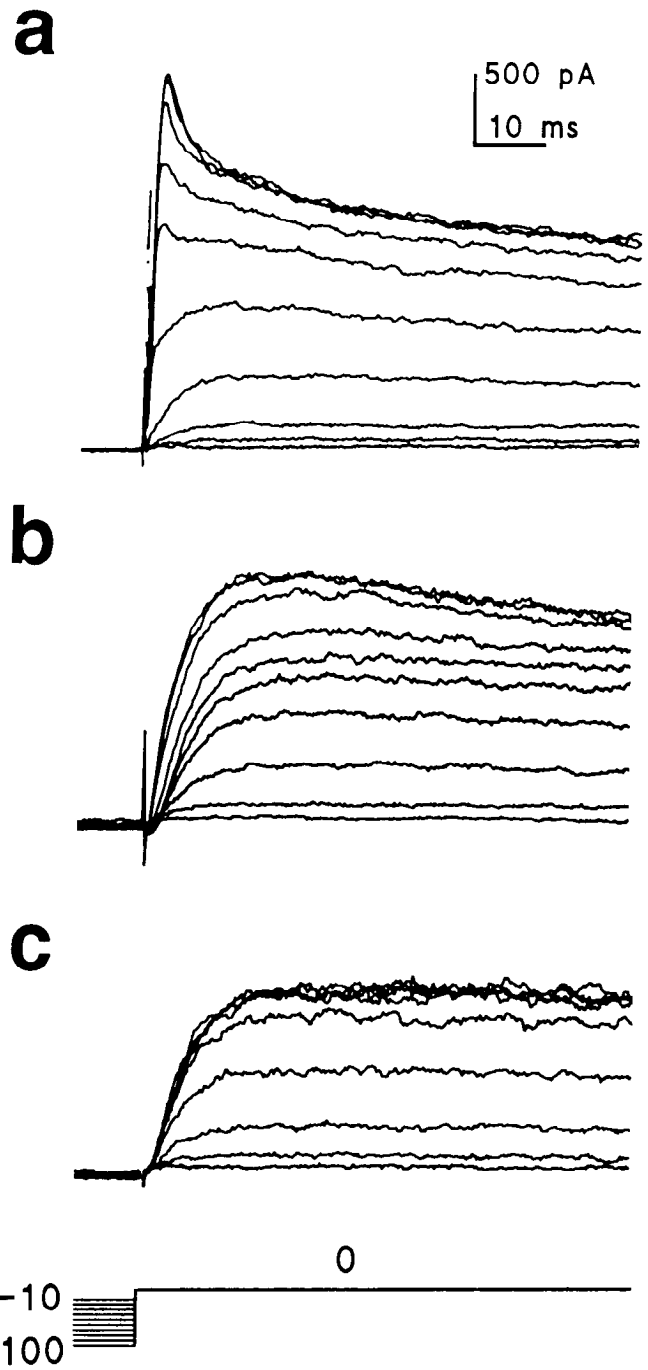

Figure 2. Three classes of outward current in *Drosophila* photoreceptors. Whole-cell recordings from pupal ommatidia demonstrating at least three major components of outward current. The same protocol of hyperpolarizing prepulses (800 msec, −10 to −110 mV in 10 mV steps) has been used throughout. *a*, Increasing hyperpolarizing prepulses elicit first I_{K_s} and then I_A and I_{K_f} (*sevenless*, p14 ommatidium). *b*, Similar protocol in an Sh^{K82a} fly (p11) more clearly reveals the second delayed rectifier component (I_{K_f}) with more hyperpolarized prepulses. Notice that this component shows significant inactivation on this time scale. *c*, In another fly (Sh^{K82a}, p9), only I_{K_s} is present, showing no inactivation on this time scale.

this observation strongly suggests a spatial segregation of the three types of channel, with the non-*Shaker* (delayed rectifier) channels presumably concentrated on the inaccessible lumen surface of the photoreceptor (Fig. 1). I_A can also be studied in relative isolation in whole-cell recordings of later-stage pupae (p11–p15) at voltages below −30 mV or in the presence of 100 μM quinidine, which blocks ≈90% of the delayed rectifier currents (see below).

The outward currents are voltage-dependent potassium conductances

The reversal potentials of the outward currents were clearly potassium dependent (Fig. 3), I_{K_s}, reversing at −90 mV in "physiological" solutions (195 mM K_o/5 mM K_i, $E_K = -91$ mV) and following the Nernst slope for potassium ions over the entire range measured. Reversal potentials shifted to near E_K almost immediately (within seconds) following solution changes. Assuming the I_{K_s} channels are concentrated on the photoreceptor's lumen surface (see above), this finding indicates that the lumen has free access to the bath solution. The reversal potential of I_{K_f} was not determined in isolation; however, reversal potentials measured in cells showing both I_{K_f} and I_{K_s} were not significantly different from those expressing I_{K_s} alone. With respect to I_A, apart from the two data points in Figure 3, in two of the most commonly used configurations, currents were inward with 200 mM K_o/5 mM K_i and outward with 5 mM K_o/200 mM K_i, but in neither case was it possible to detect reversed currents (reversal potential beyond ±70 mV).

None of the three currents showed any obvious dependence upon Ca^{2+} ions. The behavior of A-channels in inside-out patches was apparently the same whether perfused with 10 nM or 1.8 mM Ca^{2+}. Both delayed rectifier currents were routinely recorded in the whole-cell configuration using 5 mM EGTA and free Ca^{2+} buffered to ≈10 nM Ca^{2+} in the pipette and 1.8 mM Ca^{2+} in the bath. In control experiments using only 150 μM EGTA (no added Ca) in the pipette and either high (20 mM) Ca^{2+} (plus 4 mM Mg) or 0 Ca^{2+} (0.5 mM EGTA, no added Ca and 14 mM Mg to stabilize the membrane) in the bath, no systematic differences were observed in either current, beyond slight shifts (<10 mV) in voltage operating range attributable to surface charge. No voltage-sensitive inward currents were detected in these cells.

The A-current

General features. The photoreceptor A-current (I_A) closely resembles its counterpart in muscle; however, it differs in having a markedly more negative voltage operating range (Hardie et al., 1991). In inside-out patches, threshold for activation is around −90 mV, and in order to remove inactivation completely, measurements must be made from holding potentials of at least −100 mV. Averaged channel openings recorded with normal potassium concentrations reveal the typical rapid activation and inactivation kinetics of this channel (Fig. 4). As previously reported (Hardie et al., 1991), a run-down phenomenon of the current measured in patches is a progressive decrease in the amount and rate of inactivation. However, the maximum current that can be elicited is often very stable even in inside-out patches exposed to normal bath Ringer. Many patch-clamp measurements were performed using high (200 mM) K in the electrode in either the cell-attached or inside-out configuration (e.g., Fig. 4*c*). In this situation, when currents are inward at most voltages used, voltage dependence and macroscopic activation and inactivation rates are unaltered; however, the degree of inactivation is less.

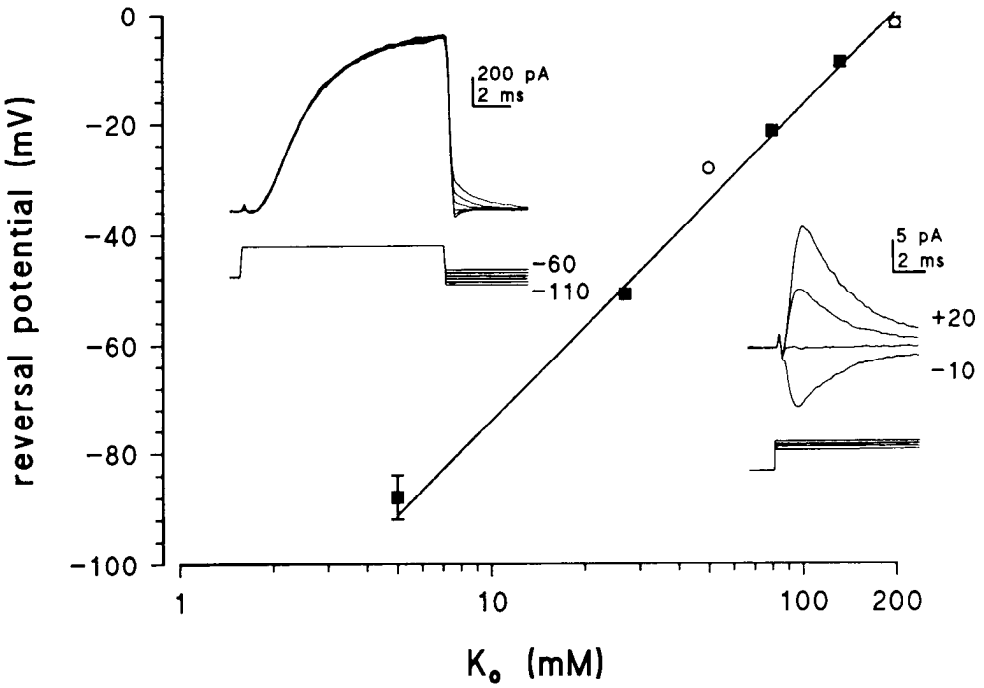

Figure 3. Reversal potentials as a function of extracellular K concentration. *Squares,* reversal potentials measured from instantaneous *I–V* curves of tail currents in whole-cell recordings of I_{K_s} (e.g., *left inset* with "physiological" 5 mM K_o, tail currents between −60 and −110 mV). *Open circles,* reversal potentials for I_A determined from averaged channel openings in multichannel patches (*e.g., right inset* with symmetrical 200 mM $K_{i/o}$, −10, 0, +10, +20 mV). K_i was 200 mM in every case. *Solid line,* Nernst slope for potassium ions. *Data points* are averaged from between 2 and 10 cells/patches. Where *error bars* (±SD) are not visible, they are smaller than the data symbols (except for the I_A data point at 50 mM K_o, which is based on two patches only).

Voltage dependence of activation. The voltage activation curve could only be accurately measured using elevated extracellular potassium, since threshold is near the normal reversal potential, and because tail currents cannot be reliably detected using low extracellular potassium. The fraction of the conductance activated by a given voltage was measured both from instantaneous tail currents and from chord conductances (g) calculated from the peak currents when the patches were exposed to known (usually symmetrical) K concentrations, using the relationship

$$g = I/(E - V). \quad (1)$$

In the latter case, the reversal potential (E) was measured directly for each patch. For instantaneous tail measurements, single exponential functions were fit to the tails and extrapolated back to the time of the voltage step. A correction was then applied for the amount of inactivation that had occurred during the activating pulse. Both methods yield similar results, and the relationship between the fraction of conductance activated (g/g_{max}) and voltage (V) is shown in Figure 5, fitted with a Boltzmann distribution of the form

$$g/g_{max} = 1/\{1 + \exp((V_{50} - V)/s)\}, \quad (2)$$

where V_{50} is the voltage at which half the channels are activated, and s (mV) is a factor determining the slope.

As is typical for A-currents, activation follows a steep sigmoidal time course indicative of multiple closed states before channel opening. The kinetics are most simply described by the time to peak (Fig. 5); although shifted to more negative voltages, these are in a similar range to those for A-currents reported in *Drosophila* muscle (10–20 msec near threshold to near 1.0 msec with saturating voltages).

The voltage dependence of the channel closing rate was also measured from tail currents (Fig. 6). Tail current relaxation has apparently not been previously measured for the *Shaker* A-current but is readily determined in macropatches using high K in the electrode. The tail currents decay with a single exponential time course, the time constant of which (τ_{rel}) shows a clear voltage dependency, decreasing from ≈2 msec at −90 mV to 0.25 msec at −150 mV. The voltage dependence of τ_{rel} is well approximated by a single exponential with an e-fold change per 26 mV. Although relaxation measurements could not be made beyond −80 or −70 mV because of interaction with channel activation and inactivation, τ_{rel} appears to become voltage independent above −90 mV (Fig. 6). Furthermore, the mean burst duration of the channels (which might be expected to equal τ_{rel}) is essentially independent of voltage from −90 to +50 mV (see Fig. 8*b* and below).

Inactivation. The steady-state inactivation curve is also shifted to similar negative voltages in comparison with the muscle A-current (Fig. 7). Although the slope of the voltage dependence (Table 1) corresponds closely with measurements in muscle, V_{50} (−83 mV in inside-out patches) is some 40–50 mV more negative than that reported in muscle or in oocyte expression studies of *Shaker* channels (Salkoff and Wyman, 1983; Iverson and Rudy, 1990; Zagotta and Aldrich, 1990).

A number of studies have highlighted differences between voltage dependence determined in patches as opposed to whole-cell recordings (e.g., Fenwick et al., 1982b; Fernandez et al., 1984). Although whole-cell recordings from pupal photoreceptors include at least two voltage-sensitive currents, I_A can be studied in relative isolation by making measurements in cells lacking I_{K_f} at −30 mV or below, where I_{K_s} is hardly activated (e.g., Fig. 7*a*, right inset): V_{50} values determined in whole-cell recordings were very consistent (−69 mV), with no difference being detected between cells that still responded to light and those in which the light response had run down. Although these values are ≈10–15 mV more positive than in patch recordings, they are still much more negative than values reported from *Shaker* channels in muscle or oocyte expression studies, and coincide with values determined with single-electrode voltage clamp from photoreceptors in the intact retina (Hardie et al., 1991; S. B. Laughlin, unpublished observations).

The most significant differences between *Shaker* channels coded for by different transcripts in oocyte expression studies

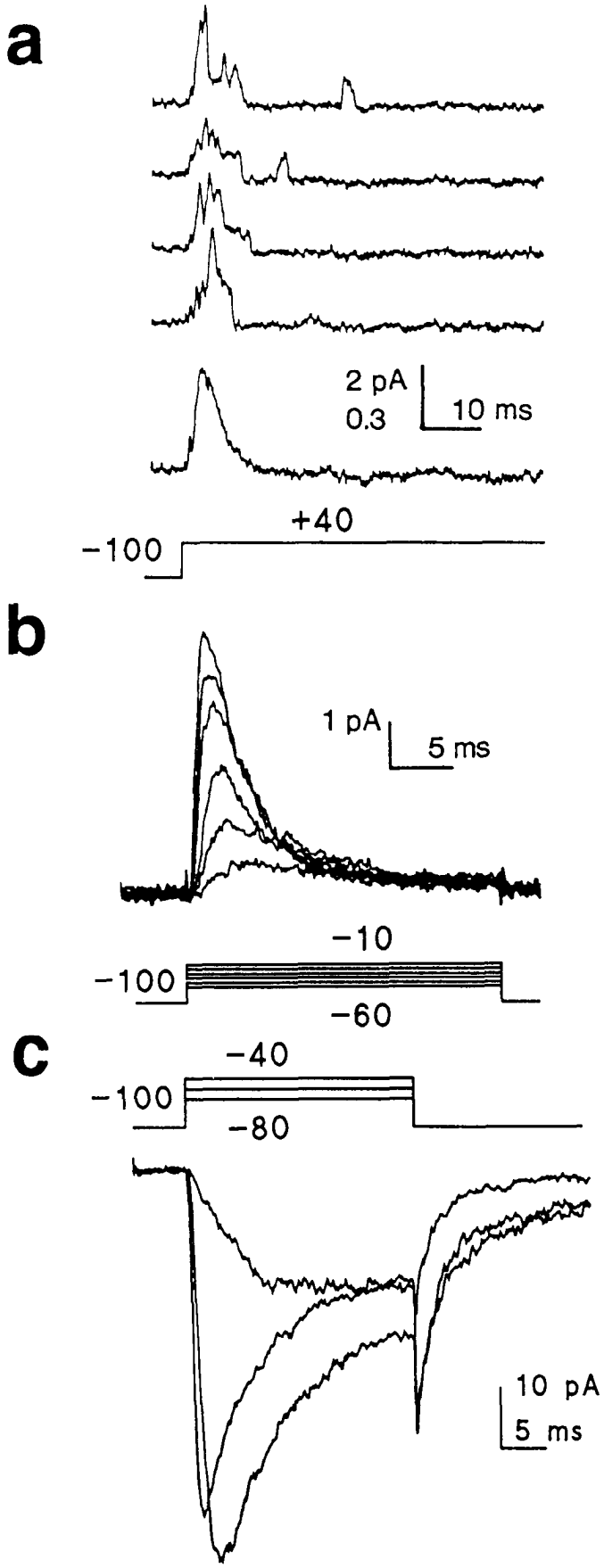

Figure 4. A-channel ensemble averages. Channel openings from multichannel cell-attached patches of adult, wild-type photoreceptors. *a*, A rare patch with only four or five active channels activated by stepping from −100 to +40 mV. The *bottom trace* is an ensemble average of 16 voltage steps. Maximum open probability is only ≈0.5 (see scale bar). "Physiological" K concentrations (200 mM K_i/5 mM K_o) were used. *b*, A family of ensemble averages ($n = 20$ sweeps) from a patch containing at least 10 channels. Rapidly inactivating outward currents are produced from a holding potential of −100 mV; voltage commands in 10 mV steps from −60 to −10 mV (200 mM K_i/5 mM K_o). *c*, Cell-attached patch containing ≈100 channels recorded with high K (200 mM) in the electrode and bath; from a holding potential of −100 mV, large inward currents are produced with voltage steps to −80, −60, and −40 mV; $n = 20$ sweeps. On-line leak subtraction has been applied to all averages, using templates below −100 mV between each cycle of the averaging protocol.

concern the rates of inactivation and recovery from inactivation (Timpe et al., 1988; Iverson and Rudy, 1990). As is also the case for muscle A-currents, the macroscopic inactivation rate of photoreceptor I_A is very rapid, with a first-order time constant (τ_{inac}) of 2–4 msec at 0 mV and above. There was some variability in this parameter, which probably reflects the tendency for τ_{inac} to increase during rundown. Presumably therefore the shorter time constants are more representative, and in whole-cell recordings the inactivation time constant at 0 mV averages 2.2 msec (±0.3; $n = 11$). In some patches, at least two exponentials were required to fit the time course of inactivation; although this may represent a run-down phenomenon, it should be noted that most *Shaker* channels expressed in oocytes also inactivate with at least two time constants (Iverson and Rudy, 1990).

Although inactivation was almost complete, a small maintained component of between 1% and 5% was always observed. This was measured in patches directly from channel open probability in the "steady state" some seconds after activation with "physiological" potassium ion distribution (5 mM K_o/200 mM K_i). As already mentioned, for inward currents recorded with high external K in the patch electrode, residual channel activity following inactivation was significantly greater with a substantial, voltage-dependent maintained component (≈30% at −60 mV and 15% at 0 mV).

Recovery from inactivation, determined in two pulse experiments, was rapid (time constant, 70–150 msec) and voltage dependent (Fig. 7*b*). Only first-order time constants were determined by fitting single exponentials to the data, although there may be a second slower component (e.g., Wu and Haugland, 1985; Iverson and Rudy, 1990). The necessity of signal averaging many sweeps made the accurate determination of slower processes impractical in patches. However, in two whole-cell recordings with negligible contribution from delayed rectifier conductances, the recovery time courses could be well fit by single exponentials (Fig. 7*b* inset).

Single-channel analysis. The high density of channels hinders rigorous single-channel analysis. Nevertheless, it is possible to extract several important parameters from multichannel patches, including the burst duration and single-channel conductance.

Burst durations were measured from continuous records of single-channel activity in the steady state. In normal (low K_o/high K_i) solutions, channels were sampled at 0 and +50 mV from the 1–5% residual activity following inactivation. In high-K_o solutions, channel activity could be measured very close to threshold (−95 to −70 mV) when little inactivation had taken place. As has been reported for A-channels in embryonic myotubes (Zagotta and Aldrich, 1990), the burst duration was essentially independent of voltage, and the distributions could

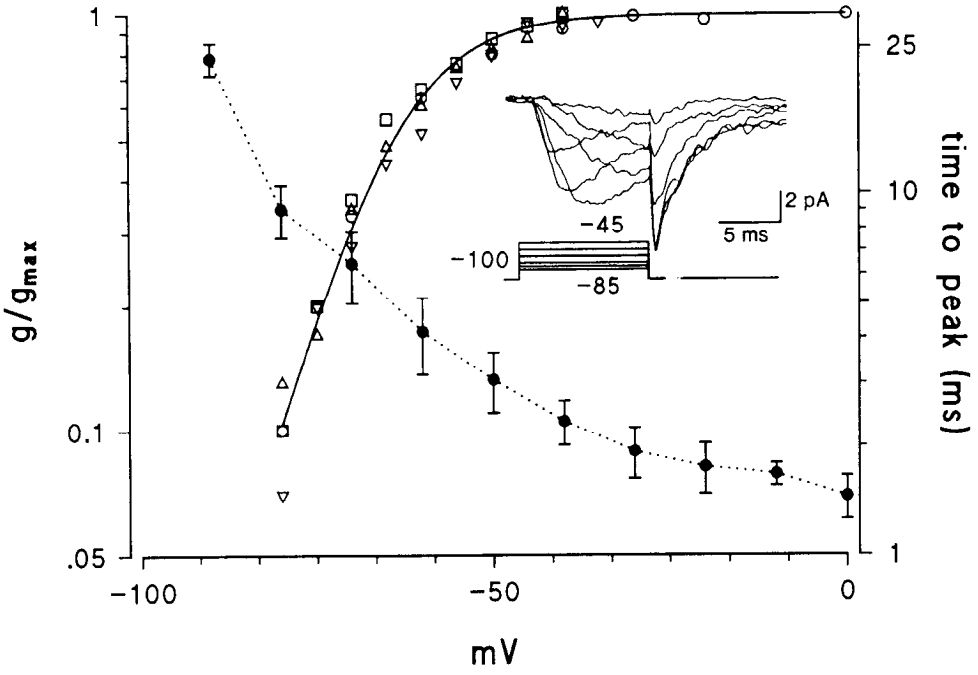

Figure 5. Activation of A-channels. *Inset,* Averaged channel openings from a multichannel inside-out patch from a holding potential of −100 mV to −85, −80, −75, −65, −55, and −45 mV. High (200 mM) K was used in the pipette so that currents are inward. On-line peak subtraction has been applied. Normalized conductances, estimated from the tail currents and corrected for the degree of inactivation (or activation), are plotted against the voltage command for four different cells on a semilog plot (*open symbols*). The data have been fit with a Boltzmann distribution (*solid curve*; Eq. 2) with V_{50} −64 mV and slope factor −7.4 mV. Similar data were also used to extract the time to peak (●), which is plotted as a function of voltage on the same graph. Each *point* is the average of between 10 and 20 patches (±SD), except for the points at −90 mV (n = 3) and 0 mV (n = 7).

often be well fit by a single exponential (e.g., Fig. 8*a*), indicating the existence of one major open state with no voltage dependence of the closed–open transition above −90 mV (Fig. 8*b*). Nevertheless, at more negative potentials the relaxation time constant shows a clear dependence upon voltage (Fig. 6), indicating that in this range the closing rate constant is indeed voltage dependent. Consistent with the observed increase in macroscopic τ_{inac} during rundown, open time distributions determined several minutes after seal formation often revealed a second, longer-lived class of openings. Since these recordings were from multichannel patches, it is not clear whether these represent a second open state or simply a subpopulation of channels that have run down.

Single-channel conductances. The single-channel slope conductance was estimated from amplitudes determined at several voltages using cursor measurements of well resolved openings. Values for outward currents measured in physiological solutions (5 mM K_o/200 mM K_i) were in the range previously reported for muscle A-channels (9–12 pS). In symmetrical (200 mM $K_{i/o}$) solutions, the single-channel I–V curve shows a marked rectification, with a slope conductance of 19 pS being measured for reversed (inward) currents (Fig. 8*c*).

Channel density and development. Channel density was quantified from the peaks of the ensemble averages to saturating voltage protocols assuming a maximum open probability of 0.5 (see Fig. 4) and the appropriate single-channel current (Fig. 8*c*). Patch area was estimated from the capacitance difference determined on embedding the electrode into a Sylgard tool in the bath (Sakmann and Neher, 1983). Although the large SD (expected with random channel distribution) renders accurate estimates impossible without large samples, it appeared that channel density increased approximately twofold during the first week of adult life. In mature (>1 week) wild-type adults, the average density was 9.3 ± 7 channels/μm^2 (n = 51), while for flies 1–6 d old channel density was 4.6 ± 4 channels/μm^2 (n = 34). With an average patch area of 4 ± 0.8 μm^2, this means that the number of channels per patch in mature flies averages ≈40, and patches with over 100 (maximum, 500) were frequently encountered.

The development of the A-current during pupal life was also investigated, in this case using whole-cell recordings. This survey was originally undertaken with the expectation that the A-current might be isolated at a sufficiently early developmental stage, as is the case in pupal muscle (Salkoff and Wyman, 1981a, 1983). However, it turns out that in the photoreceptors, the two delayed rectifier currents develop before the A-current. I_{Kf} and

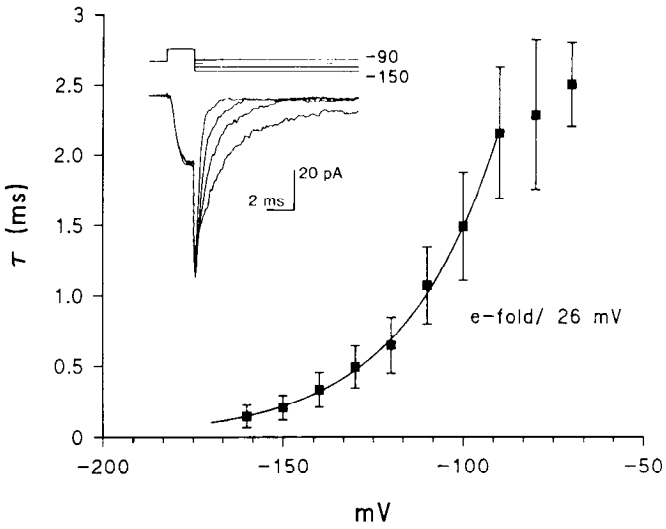

Figure 6. Relaxation of tail currents in multichannel patches. The *inset* shows averaged channel openings to voltage protocols involving steps to increasing hyperpolarizations at the peak of the current induced by a voltage step to −30 mV. Currents were recorded with high (200 mM) external K so that all currents are inward and were leak subtracted on line. The relaxation time courses were well fit by single exponentials, the time constant of which is plotted as function of voltage. The *curve* drawn through the points is itself a single exponential with no residual component and a slope of e-fold/26 mV. *Data points* (±SD) are averaged from between 10 and 20 patches.

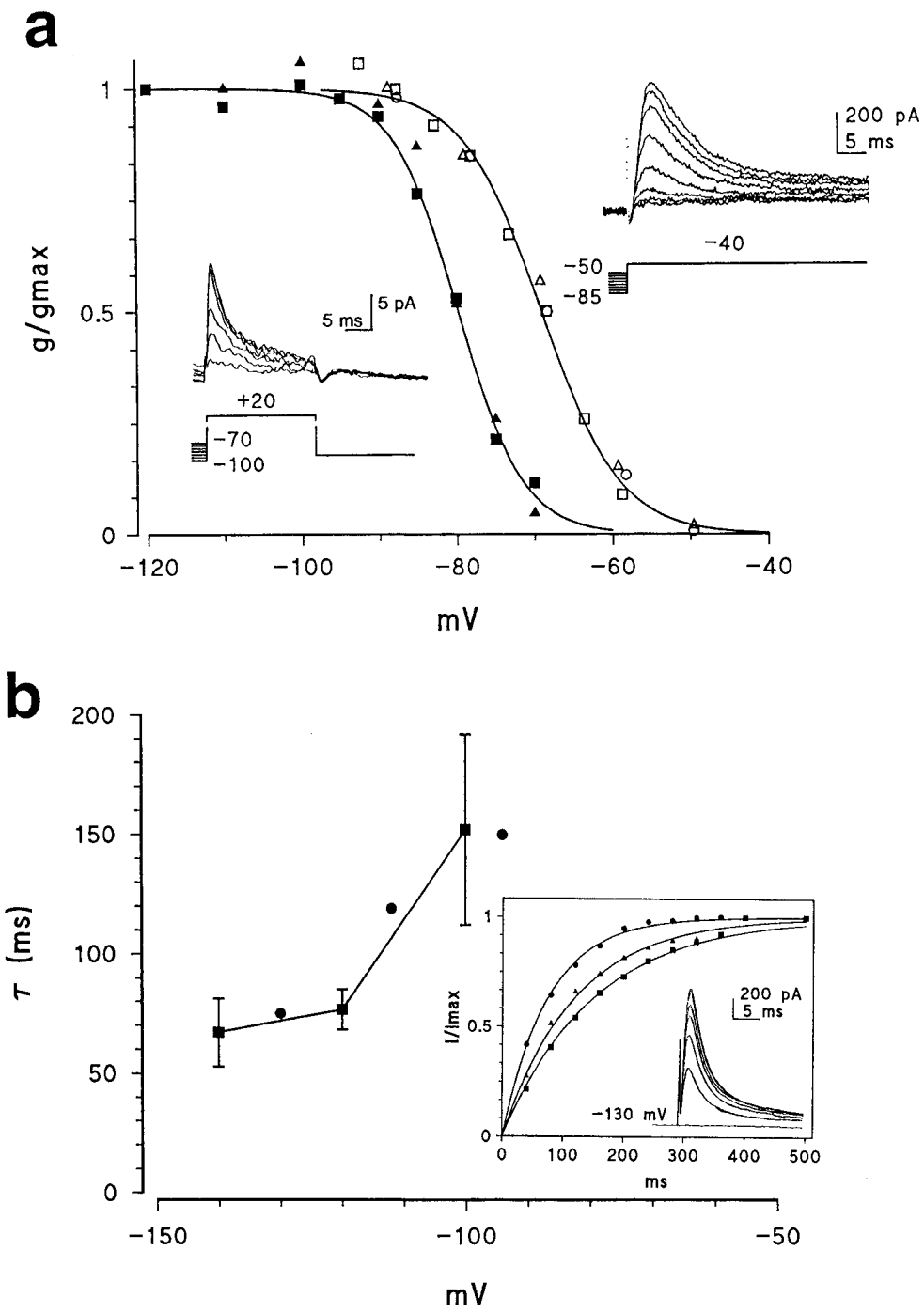

Figure 7. Voltage and time dependence of removal of inactivation. *a:Left inset,* Averaged channel openings from an inside-out patch at +20 mV following 1 sec prepulses between −70 and −100 mV (5 mV steps). "Physiological" K solutions have been used (5 mM K_o, 200 mM K_i). *Right inset,* I_A recorded in whole-cell recording (wild-type p15 photoreceptor) at −40 mV following prepulses between −50 and −85 mV (5 mV steps). The normalized conductances of two patches (*solid symbols*) and three whole cells (*open symbols*) are plotted as a function of the prepulse voltage and fitted with Boltzmann curves (Eq. 2) of slope 4.2, V_{50} −79 mV (patch) and slope 4.9 mV, V_{50} −69 mV (whole cell). *b,* Recovery from inactivation. The *inset* shows a whole-cell recording of a photoreceptor in which I_A dominated the whole-cell current, elicited at 0 mV following prepulses (−130 mV) of increasing duration (20–140 msec). The *curves* are single exponential functions (τ = 75, 119, and 150 msec) fitted to the normalized peak currents (I/I_{max}) following prepulses to three different holding potentials (−130, −110, and −95 mV). The time constants for recovery from inactivation (τ) of this cell are plotted on the *main graph* as a function of prepulse potential (*circles*) along with averaged data (±SD) collected in a similar manner from five cell-attached patches (*squares*).

Table 1. Properties of voltage-sensitive potassium conductances in *Drosophila* photoreceptors

			Inactivation (mV)		Activation (mV)	
	t-pk (msec)	τ_{inac} (msec)	V_{50}	*s*	V_{50}	*s*
I_A	1.8 ± 0.3	2.2 ± 0.3	−69 ± 5	4.7 ± 0.9	−48 ± 7	−9 ± 3
	(20)	(11)	(26)	(18)	(33)	(33)
I_{Kf}	6.8 ± 2	76 ± 50	−81 ± 4	4.7 ± 0.3	−38	−7
	(8)	(26)	(9)	(9)	(2)	(2)
I_{Ks}	11.3 ± 1.1	442 ± 69	−41 ± 3.5	6.8 ± 0.8	−12 ± 6.6	−7.1 ± 2.2
	(11)	2043 ± 330[a]	(19)	(28)	(12)	(12)
		(9)				

All values are presented as means ± SD (number of cells in parentheses). Data for the delayed rectifier conductances, I_{Ks} and I_{Kf}, are from pupal whole-cell recordings. Voltage dependencies (V_{50} values) for I_{Ks} are from dark-adapted cells that still showed responses to light. Values for I_A are from patches from adult photoreceptors except for τ_{inac} and inactivation V_{50} values, which are from pupal whole-cell recordings. In addition, the activation V_{50} of I_A (determined in patch recordings) has been shifted by +15 mV, that is, the estimated discrepancy between patch and whole-cell recordings (see Results). Times to peak (*t*-pk) were measured with near-saturating voltage steps, that is, 0 mV (I_{Kf} and I_A) or +20 mV (I_{Ks}). Inactivation time constants (τ_{inac}) were all measured at 0 mV. *s* = slope factor (Eq. 1).

[a] For I_{Ks}, τ_{inac} values were fit with two exponentials, the slower component accounting for 31% (±10%) of the current.

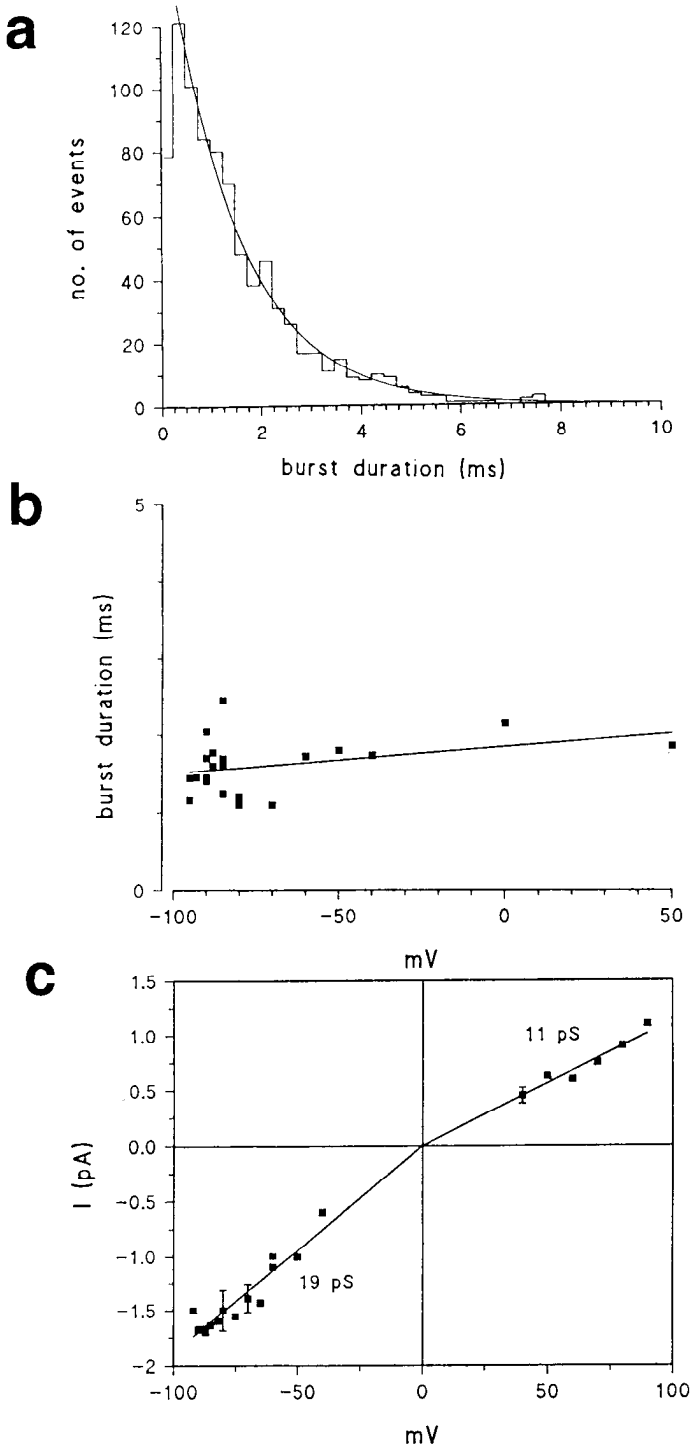

Figure 8. Single-channel properties of *Shaker* A-channels. *a,* Burst duration distribution histogram for A-channels recorded in a multi-channel patch at −90 mV with high (200 mM) K_o. Bursts have been defined as groups of openings separated by closed times of less than 1 msec. The distribution has been fit with a single exponential with time constant 1.45 msec (ignoring the initial low-count bin). Data sampled at 20 kHz, filtered at 2 kHz. *b,* Mean burst durations (estimated by fitting single exponentials to the distributions, as above) plotted as a function of voltage. There is no obvious dependence of this parameter on voltage in the measured range (−90 to +50 mV). Measurements are from 17 patches showing a single major component to the burst duration distribution, recorded with both high (200 mM) and low (5 mM) K_o. In five of these patches, measurements were made at two holding potentials (e.g., 0 and 50 mV, −90 and −60 mV), otherwise only at one potential near threshold. *c,* Single-channel *I–V* relationship determined with 200 mM K on either side of the membrane. Channel amplitudes determined by cursor measurements of well resolved openings. Slope conductances determined by regression lines (constrained to pass through the origin) show significant rectification (19 pS for inward currents and 11 pS for outward currents). Data (±SD) are from seven perfused inside-out patches.

I_{Ks} were both observed at the earliest stage examined (late p8 = ≈60 hr), while I_A first became apparent between stages p11 and p12 (≈75 hr; e.g., see Fig. 15). The maximum A-current that could be elicited (at 0 mV) developed rapidly from around 100 pA at stage p11 to more than 4 nA at stage p15 (>90 hr).

The delayed rectifier currents I_{Ks} and I_{Kf}

As described above, both the delayed rectifier currents, I_{Ks} and I_{Kf}, were investigated in whole-cell recordings from dissociated pupal ommatidia. Most measurements were made using *Shaker* mutants (Sh^{KS133} and Sh^{K82a}); however, wild-type pupae were also used up to stage p10/11, that is, before I_A has developed to any extent.

In ≈30% of recordings from pupal photoreceptors in *Shaker* mutants, both delayed rectifier–type conductances were obviously present, as most clearly seen with an inactivation prepulse protocol (see Figs. 2*b,* 9*a,* 12*b*). A slowly inactivating current is recruited following prepulses to between −10 and −60 mV, and a second, more rapidly inactivating component becomes apparent with more negative prepulses. The steady-state inactivation curve for such data (Fig. 9*a*) is well fit by the weighted sum of two Boltzmann distributions (weighting factor b):

$$g/g_{max} = 1/\{1 + \exp((V_{50} - V)/s)\} + b/\{1 + \exp((V'_{50} - V)/s')\}. \quad (3)$$

Activation protocols similarly reveal two components: from holding potentials of −60 mV only I_{Ks} is recruited, but from −80 mV two kinetic components can be detected (Fig. 9*b*). The corresponding activation curves clearly show the more positive activation range of the more slowly inactivating current.

I_{Ks} was often the only voltage-sensitive conductance detected in young pupal or *Shaker* photoreceptors (70% of recordings) and could be well characterized in isolation. I_{Kf} appeared rather labile under these experimental conditions. When present, it accounted initially for only 23% (±14%; n = 44) of the total non-*Shaker* current and then often ran down over a period of 10–30 min. Nevertheless, in a very small number of cells (four) I_{Kf} was the only, or dominant, current present. Correspondingly, its properties have not been analyzed in such detail. For ease of comparison, the limited data available are presented alongside those of I_{Ks}.

Voltage dependence of activation and inactivation. During prolonged whole-cell recording, the apparent voltage operating range of I_{Ks} drifted in a negative direction, typically reaching "end" values 10–20 mV more negative after 15–30 min. While this drift may include a component due to the dissipation of a Donnan equilibrium between the chloride of the electrode and the large organic intracellular anions (Marty and Neher, 1983; Fernandez et al., 1984), a number of observations suggest a change in the state of the channels, or their immediate environment. First, in recordings made *without* Mg-ATP in the electrode, the drift was usually more pronounced (Fig. 10*b*); second, the drift appeared to be channel specific—I_A, for example, was much more stable, with inactivation V_{50} values drifting by less than

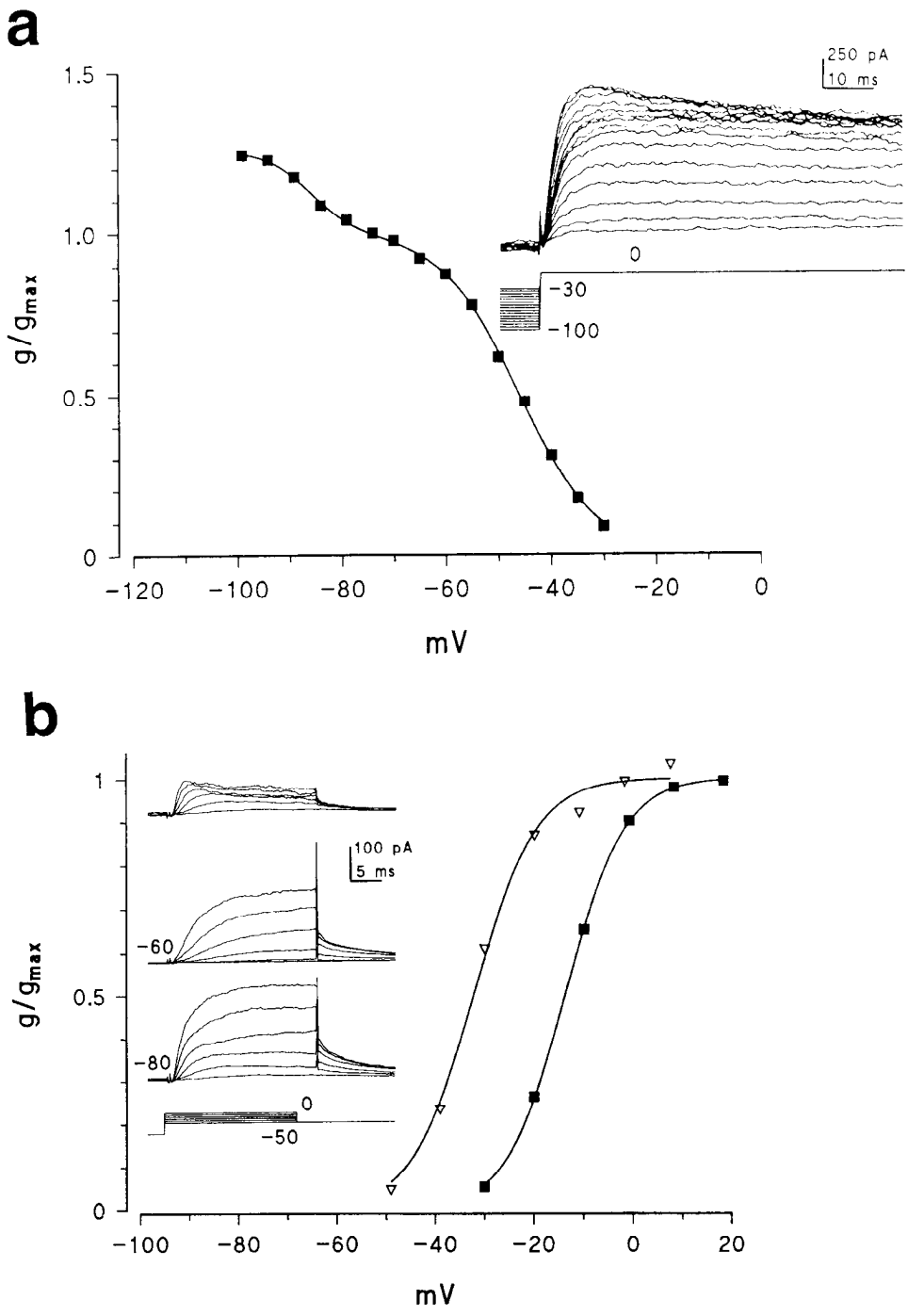

Figure 9. Delayed rectifier conductances in pupal whole-cell recordings. *a:Inset,* Whole-cell currents at 0 mV following increasing hyperpolarizing prepulses (800 msec, −30 to −100 mV, 5 mV steps) in an Sh^{KS2A} p11 photoreceptor. Following prepulses below −60 mV, a second more rapidly inactivating outward current (I_{Kf}) is recruited. Peak currents, normalized to maximum I_{Ks} current (determined by curve fitting), have been plotted against prepulse voltage. The resulting voltage dependence of inactivation clearly shows the two components and has been fit by the weighted sum of two Boltzmann distributions (Eq. 3) with V_{50}, −46 mV; s, 7.3 mV; V'_{50}, −86 mV; s', 4.3 mV; and b (proportion of current attributable to I_{Kf}), 0.26. *b:Inset,* Activation series from a holding potential of −60 mV (*middle*) reveals only one component (I_{Ks}) with an activation threshold near −30 mV; *below,* from a holding potential of −80 mV, both I_{Ks} and I_{Kf} are recruited, and activation threshold is now −50 mV. Subtracting the two families of currents (*top*) reveals I_{Kf} alone. The *graph* shows the normalized conductances determined from the tail currents (I_{Ks}, ■) or the peaks (I_{Kf}, ▽).

5 mV; third, in a number of cells recorded in high (50–80 mM) external K, the reversal potential for I_{Ks} was monitored repeatedly and found again to drift by less than 5 mV, reaching the expected E_K value within 5 min; finally, V_{50} values from photoreceptors recorded in the dark, and which still showed responses to light, were significantly more positive and less variable (V_{50} = −41 ± 3.5 mV; n = 19) than those in which the light response had run down (V_{50} = −50 ± 8 mV; n = 30). These observations raise the interesting possibility that the voltage dependence of I_{Ks} in photoreceptors may be subject to modulation, for example, as a function of light adaptation.

The voltage dependences of activation and inactivation for both I_{Ks} and I_{Kf} are summarized in Figure 10 and Table 1. V_{50} values for I_{Ks} are from cells that still showed responses to light, measured at least 5 min after establishing the whole-cell configuration. The steady-state inactivation curve for I_{Kf} lies ≈40–50 mV more negative and in addition has a steeper voltage dependence. The voltage dependence of activation for I_{Kf} was only determined in two cells, yielding V_{50} values of −45 and −30 mV, respectively.

Similar recordings (e.g., Fig. 11) were used to extract the time constant of activation and its dependence on voltage, traces being fitted with a power function of the form

$$I_t = I_\infty(1 - e^{-t/\tau})^n. \quad (4)$$

For the sake of presentation, the time constants (τ) plotted in

Figure 11 are all based on curve fits assuming an exponent (n) of 2. However, data were variable in this respect, and even when considering only records with minimal series resistance errors (<1 mV), an exponent of 3 or 4 gave better fits in some cells. Relaxation time constants were measured from the tail currents (Fig. 11, left inset) at different voltages and plotted on the same figure. To enhance their size, these tail currents were recorded with elevated external K. Two particle gating has also been assumed for these values (i.e., the values plotted are *twice* the actual single exponential time constants derived from the traces).

The corresponding time constants for I_{Kf} have not been comprehensively characterized, but the limited data on activation time constants are intermediate between I_A and I_{Ks} (Fig. 11, Table 1). For direct comparison, the time constants in Figure 11 are also based upon fits to Equation 4 with $n = 2$, although no confidence is attributed to this value.

Inactivation. As is the case for delayed rectifier–type conductances reported in *Drosophila* neurons and muscles (e.g., Solc and Aldrich, 1988; Zagotta et al., 1988), the photoreceptor delayed rectifier conductances also inactivate, but much more slowly than the A-current. There is still a measurable (5–10%) maintained outward current at least 10–20 sec following activation. Although this may include a contribution from I_{Ks} channels that have not inactivated completely, the existence of a third class of slowly or noninactivating voltage-sensitive K channel is suggested by pharmacological evidence (see below).

I_{Ks} usually decayed with a double exponential time course. The faster component has a time constant (τ_{inac}) of ≈500 msec, while τ_{inac} for the slower component was in the range 1–3 sec. There is apparently little voltage dependence in the measured range (−40 to +20 mV); however, the contribution of the slower component usually increased with depolarization, possibly indicating an increased contribution from a non- or very slowly inactivating K channel. To test whether observed inactivation includes a component due to potassium ion accumulation or depletion, the time course of the conductance change during inactivation was monitored using a "ripple" consisting of 10 Hz, 20 mV square wave pulses superimposed upon the voltage protocol. The results could be fit by exactly the same time course that best described the current decay in the absence of ripple, although the resolution of the data was no longer sufficient to decide whether both exponential components were required.

The time course for the recovery from inactivation was followed in two pulse experiments as detailed above for I_A. The results are well fit by single exponential time course with a voltage-dependent time constant summarized in Figure 13.

Inactivation of the more rapidly inactivating delayed rectifier conductance was followed both in the few cells expressing this component alone (e.g., Fig. 12*c*) and in cells expressing both components by subtraction of the slower component (e.g., Figs. 9*b*, 12*b*). This can be conveniently performed by measuring outward currents at the same voltage, first following a prepulse to ≈−60 mV, which completely removes inactivation of I_{Ks}, while leaving I_{Kf} almost completely inactivated, and then following a prepulse to −80 mV or below, which removes inactivation of both components. In cells expressing only I_{Ks}, this protocol results in essentially identical current waveforms. I_{Kf} appears to inactivate completely with a single exponential time constant of ≈75 msec (Table 1). There was some indication that the rate of inactivation of I_{Kf} increases with pupal age (τ_{inac} extremes of 200 msec in a p8 fly vs. 30 msec in p15), but insufficient data were collected to substantiate this point.

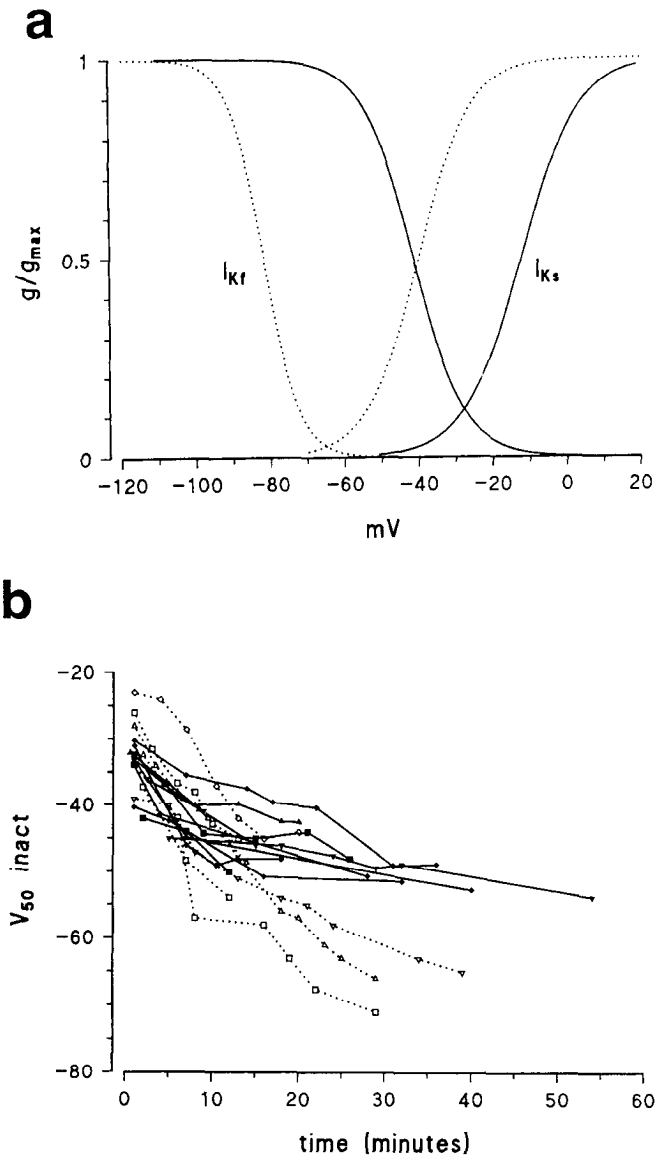

Figure 10. Voltage operating ranges of I_{Ks} and I_{Kf}. *a*, Summary diagram showing the voltage dependence of inactivation and activation for I_{Ks} (*solid curves*) and I_{Kf} (*dotted curves*). The curves are Boltzmann distributions (Eq. 2) using data tabulated in Table 1. For I_{Ks}, only data from dark-adapted cells that still responded to light have been included. *b*, V_{50} values of inactivation of I_{Ks} as a function of time after establishing the whole-cell configuration. Each line represents measurements from one cell in the presence (*solid lines*) or absence (*dotted lines*) of Mg-ATP in the electrode. All data in this plot were from cells prepared and recorded from in normal room light—that is, in which the light response had already run down.

Single channels. A search for channels corresponding to the non-*Shaker* currents was made in adult photoreceptors of *Shaker* mutants; however, it was apparent that voltage-sensitive channels were very rare on the accessible membrane (see Fig. 1). In four patches, channels were recorded that probably correspond to I_{Ks}. The limited data on these channels, which occurred as single- or two-channel patches, are summarized in Figure 14. All the patches were recorded with high (200 mM) external K in the patch pipette. Under these conditions, the single-channel conductance was 30–35 pS for reversed (inward) currents. Channel openings were characteristically long and, at

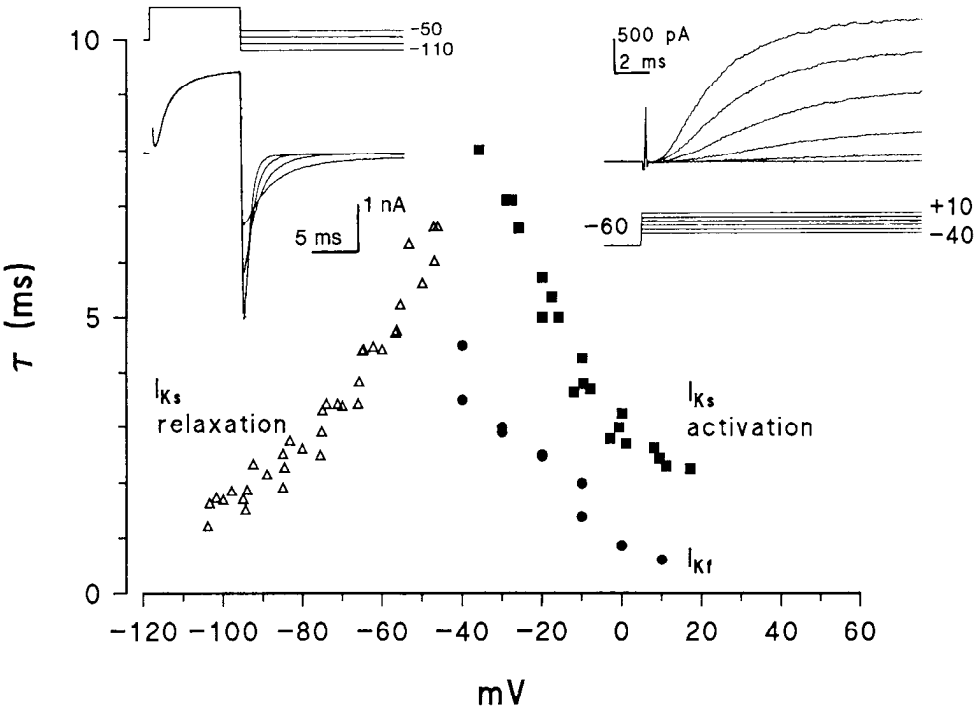

Figure 11. Time constants of relaxation and activation for the delayed rectifier currents. *Left inset,* Tail currents recorded between −50 and −110 mV in high (50 mM) external K following a voltage command inducing maximum activation in a cell with only I_{Ks}. The relaxation time courses are well fit by single exponentials. The time constants have been multiplied by two (assuming two-particle gating; see Results) and plotted as a function of voltage (*triangles*; data from five cells). *Right inset,* Activation time course of I_{Ks}. The activation time constants (*squares*; data from four cells) were obtained by fitting traces with a power function (Eq. 3) using an exponent n of 2. V_{50} values for activation of I_{Ks} in all cells used for this figure were between −15 and −20 mV ($V_{50\ inac}$, −45 to −50 mV). *Circles,* activation time constants for I_{Kf} (two cells) fitted with $n = 2$ kinetics for direct comparison.

relatively depolarized potentials (e.g., −30 mV), could last for over 1 sec. Openings were followed by a long-lived but nonabsorbing inactivated state from which reopenings could occur. Voltage dependence was not determined systematically; however, the activation time course of ensemble averages at a single voltage showed similar kinetics to whole-cell I_{Ks} currents (Fig. 14*c*) if a 15 mV allowance is made for the mismatch between patch and whole-cell voltage dependence (as for I_A, see above).

Channels with kinetics that might correspond to the more rapidly inactivating delayed rectifier conductance (I_{Kf}) were not detected.

Pharmacology

As previously described (Salkoff and Wyman, 1983; Zagotta et al., 1988), the *Shaker* A-current is blocked by millimolar concentrations of 4-aminopyridine (4-AP). In inside-out patches, channels are blocked by addition of 1 mM 4-AP to the solution bathing the intracellular surface of the patch. In whole-cell recordings, 5 mM 4-AP in the bath reduced delayed rectifier currents by less than 25%, although I_A was almost completely abolished (<5% current remaining).

As is also the case for I_K in *Drosophila* muscle (Singh and Wu, 1989), both components of the delayed rectifier conductance in whole-cell recordings of pupal photoreceptors were almost completely blocked by addition of 100 μM quinidine to the bath (Fig. 15). As has been reported in *Aplysia* neurons (Hermann and Gorman, 1984), the effect of quinidine appears to be both voltage and state dependent. The block increases during maintained depolarization resulting in currents that inactivate with a time constant of 5–10 msec at potentials above 0 mV (Fig. 15*b*). I_A is largely unaffected by the quinidine block and can be measured in relative isolation in whole-cell recordings with quinidine in the bath (e.g., Fig. 15*a*). Following application of quinidine in *Shaker* mutants, the residual outward current shows significantly less inactivation than control levels (Fig. 15*c*). This suggests that at least some of the maintained component of the outward current may represent a distinct class of noninactivating channel rather than residual activity of I_{Ks} or I_{Kf} channels.

The effect of tetraethylammonium (TEA) on the delayed rectifier currents was also tested; 50 mM concentrations in the bath reduced I_{Ks} to residual values of only 10–15% and reduced I_A to ≈25%. As was the case with quinidine, the maintained outward component was not so severely affected as the peak of I_{Ks} (20% residual compared with 13%). The effect of internal TEA was not tested. The effects of all drugs (4-AP, quinidine, and TEA) were almost completely reversible within minutes of washing.

Mutant analysis

In a parallel study, it has already been reported that I_A is absent or greatly reduced in null mutants of the *Shaker* locus, and mutations at specific loci within the *Shaker* locus were used to address the question of which transcripts are expressed in the photoreceptors (Hardie et al., 1991). One other gene, *eag,* has been reported to affect voltage-sensitive potassium channels in *Drosophila* muscle (Wu et al., 1983a). However, although not exhaustively investigated, in photoreceptors of *eag* mutants, I_A, I_{Ks}, and I_{Kf} were all present with apparently normal properties (viz., voltage dependence, rates of activation and inactivation, and amplitude; data not shown).

As in all Diptera, *Drosophila* ommatidia contain eight photoreceptors. The six largest of these (R1–6) are believed to represent a homogeneous population, but in addition there are two smaller cells (R7 and R8) with distinct functional properties (review: Hardie, 1985). Since I_{Kf} was only detected in a minority of cells, one might consider that this current may have been restricted to one of the minor photoreceptor classes. To control for this possibility, recordings were made from the mutant *sevenless,* which completely lacks photoreceptor R7 (Harris et al., 1976). By ensuring that seals were made at the distal end of the ommatidium, one can also exclude the possibility of recording

from R8, which occupies only the proximal one-third of the ommatidium (Hardie, 1985). Whole-cell recordings from these mutants included several cells (6 of 35) with $I_{K/}$ as well as I_{Ks} and I_A, thus confirming that all these currents are a property of the one cell class, R1–6 (e.g., Fig. 2*a*). The time constant of inactivation of $I_{K/}$ in *sev* flies also showed a similar variation (40–120 msec) to wild type. There remains the possibility that R7 and/or R8 may account for the very rare recordings (4 of over 200 cells), where $I_{K/}$ was the only current obviously present (e.g., Fig. 12*c*).

Discussion

Together with a parallel study (Hardie et al., 1991), the results demonstrate that it is possible to employ patch-clamp techniques to make routine measurements of both whole-cell currents and single-channel activity from an identified class of sensory neuron (photoreceptors R1–6), in a preparation consisting of dissociated *Drosophila* ommatidia. The present article documents the properties of three voltage-sensitive potassium conductances in these cells, including a novel A-current coded by the *Shaker* gene, and two classes of delayed rectifier–type conductances.

The Shaker *A-current*

The molecular/genetic potential of this preparation has been clearly demonstrated in a parallel study (Hardie et al., 1991). A combination of mutant analysis and PCR of retinal tissue provided strong evidence that the A-channels in photoreceptors are coded by multiple *Shaker* transcripts, distinct from those responsible for the muscle's A-current. This thus constituted a biological rationale for the extensive molecular diversity implicit in the structure of the *Shaker* locus.

The photoreceptor A-channels stand out from most previous studies of *Shaker* channels by their greatly shifted operating range. V_{50} for inactivation (−83 mV in patches, −69 mV in whole-cell recordings) is 30–45 mV negative to that reported in all other wild-type *Shaker* channels studied, both in the three muscle preparations (embryonic, larval, and pupal) and in oocyte expression studies (Salkoff and Wyman, 1983; Wu and Haugland, 1985; Iverson et al., 1988; Zagotta and Aldrich, 1990). This negative operating range has further been confirmed by single-electrode voltage clamp in the intact retina (Hardie et al., 1991). There are indications that such a negative operating range may in fact be the norm in the nervous system. A-currents in virtually all other neuronal preparations (including *Drosophila* non-*Shaker* A-currents) have a similar negative operating range (review: Rudy, 1988), and in the single other study describing *Shaker* currents in *Drosophila* neurons (Baker and Salkoff, 1990), V_{50} was also shifted to more negative values (V_{50} = −52 mV).

With the important exception of the voltage operating range, A-channels in photoreceptors are rather similar to those reported in muscle, and in particular, with appropriate allowance for the voltage shift, both activation and inactivation time courses are apparently indistinguishable. As previously reported (Hardie et al., 1991), one other difference detected was in the susceptibility to run down: patches from photoreceptors maintain up to 100% activity after 1 hr, while in muscle embryonic myotubes, channels run down within minutes, even in whole-cell recordings (Zagotta et al., 1989).

The developmental profiles of muscle and photoreceptor A-channels are also quite distinct. In photoreceptors, I_A was first detected at pupal stage p11 [corresponding to ≈76 hr development at 25°C (Bainbridge and Bownes, 1981)], while delayed rectifier currents were already present at the earliest stages investigated (late p8 = 60–70 hr). In muscle, the situation is apparently exactly reversed, with I_A first appearing at ≈60 hr and I_K only after 75 hr (Salkoff and Wyman, 1981a, 1983).

In the most widely accepted model of *Shaker* channel gating, there is presumed to be only one open state whose opening and closing rate constants are independent of voltage. All voltage dependence is assumed to reside in transitions within the (multiple) closed states prior to opening (Zagotta and Aldrich, 1990).

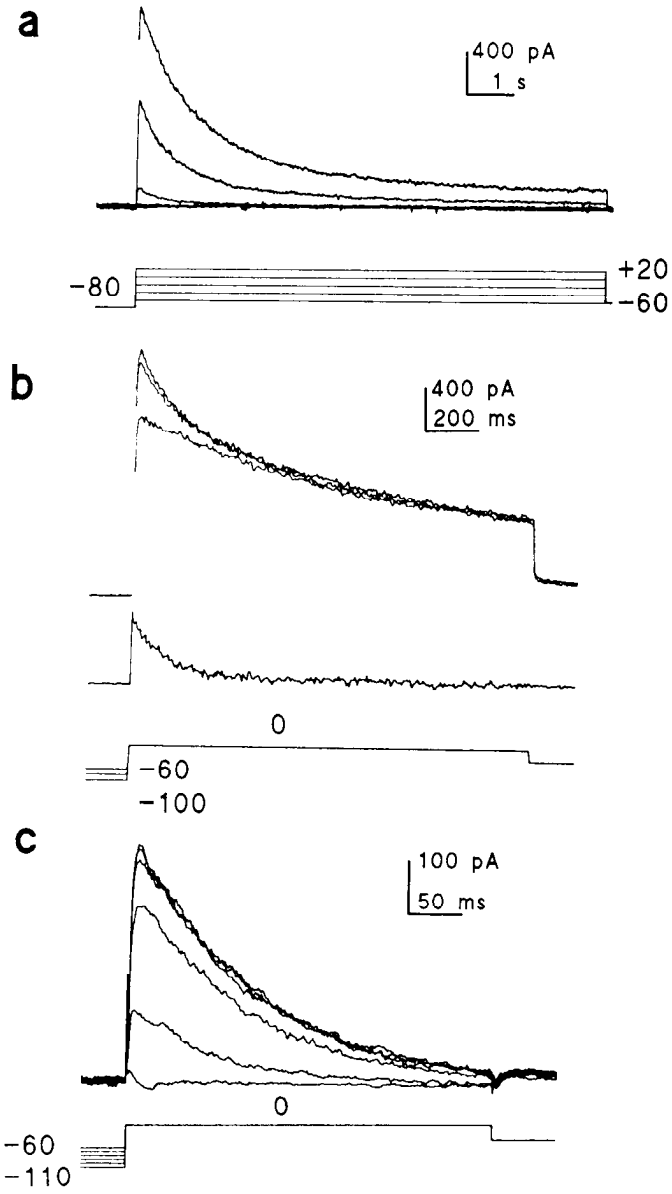

Figure 12. Inactivation of delayed rectifier currents. *a*, Currents induced by ≈10-sec voltage steps from −60 mV to +20 mV (20 mV intervals) in a cell displaying only I_{Ks}. At 0 mV, the inactivation time course could be fit by two exponentials of 608 msec (67%) and 2.5 sec (23%) with a 10% maintained component. *b*, Currents induced at 0 mV following prepulses to −60, −80, and −100 mV. The more rapidly inactivating component ($I_{K/}$) is clearly revealed with the more hyperpolarized prepulses and has been isolated in the *lower trace* by subtraction. It inactivates completely with a single exponential time course, in this case, of 120 msec. *c*, A rare cell exhibiting only $I_{K/}$, currents were measured at 0 mV following prepulses from −60 to −110 mV. The inactivation can be fit with a single exponential of 112 msec.

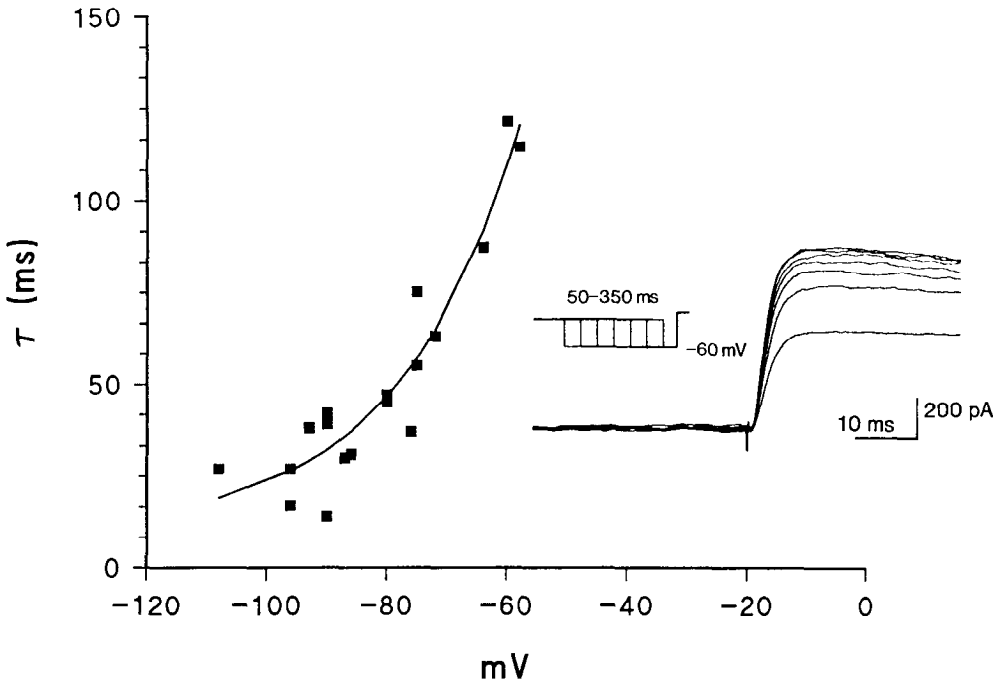

Figure 13. Recovery from inactivation for I_{K_s}. The *inset* shows how increasing the duration of a −60-mV prepulse from 50 to 350 msec completely removes the inactivation (induced by 5 sec, 0 mV interpulse intervals). The recovery from inactivation can be well fit with a single exponential function, the time constant of which is plotted as a function of voltage (data from five different cells).

While the present study confirms the independence of burst duration on voltage above threshold (−90 mV), tail current measurements indicate that below −90 mV the open–closed transition rate is strongly voltage dependent (see Figs. 6, 8*b*). There is no obvious reason to suppose that this previously undescribed feature of *Shaker* channel gating is unique to the photoreceptor A-channel, and a similar voltage dependence in other *Shaker* channels may be predicted if investigated with the appropriate solutions and protocols.

Delayed rectifier currents

Delayed rectifier conductances in *Drosophila* have previously been characterized in embryonic, larval, and pupal muscle preparations, as well as in larval cultured neurons (Salkoff and Wyman, 1981b, 1983; Wu and Haugland, 1985; Zagotta and Aldrich, 1988; Solc and Aldrich, 1989). In many respects, they show similarities both among each other and with the slowly inactivating delayed rectifier (I_{K_s}) of the present study.

In particular, when investigated at the same temperature (Solc and Aldrich, 1988; Zagotta et al., 1988), the rates of activation and inactivation are similar. V_{50} for the steady-state inactivation curve of I_K in muscle is ≈20 mV more positive than in photoreceptors; however, the slope values are similar (Salkoff and Wyman, 1983; Wu and Haugland, 1986). In larval neurons, V_{50} was very variable (−40 to −88 mV) but encompassed the values found in photoreceptors (V_{50} = −40 to −50 mV). While the variability may reflect the heterogeneous nature of the larval neuron preparation, it may also be an indication that the voltage dependence of the channels is subject to modulation as suggested in the present study. The single-channel conductance of the few presumptive I_{K_s} channels (30–35 pS for inward currents; Fig. 15) is similar to that reported for neuronal I_K channels (Solc and Aldrich, 1988). Like the *Shaker* channels (McKinnon and Yellen, 1990; Fig. 8*c*), this channel is also reported to rectify, with a conductance of only 20 pS for outward currents in symmetrical K solutions (Solc and Aldrich, 1988).

A second delayed rectifier conductance of the sort identified here (I_{K_f}) has not previously been distinguished in *Drosophila*, although its properties (Table 1) are almost encompassed in the extremes of properties reported for neuronal K_d channels by Solc and Aldrich (1988). While the relatively rapid inactivation might tempt one to classify this conductance as an A-current, inactivation is still slower than other neuronal A-currents reported in *Drosophila* (e.g., Solc and Aldrich, 1988). It also has a comparatively slow time course of activation (Fig. 7, Table 1) and, in common with other delayed rectifier conductances in *Drosophila* (Solc and Aldrich, 1988; Singh and Wu, 1989), is relatively insensitive to 4-AP but blocked by micromolar concentrations of quinidine. Indeed, in the absence of single-channel data or pharmacological separation, one cannot exclude the possibility that I_{K_f} and I_{K_s} represent two different metabolically maintained states of the same channel.

Genes coding for native delayed rectifier channels in *Drosophila* have yet to be identified. The *eag* mutation has been reported to have a limited and variable effect on muscle I_K and I_A (Wu et al., 1983a), but no apparent effect on delayed rectifier–type channels in larval neurons (Yamamoto and Suzuki, 1989). In the present study, a severe allele of this gene had no obvious effect on any of the potassium conductances in photoreceptors. Of the three *Shaker*-like genes (*Shal, Shaw,* and *Shab*) cloned by homology in *Drosophila* (Butler et al., 1989), photoreceptor I_{K_s}, at least, most closely resembles the properties of *Shal* when expressed in frog oocytes (Wei et al., 1990). Close quantitative similarities can be recognized in terms of rates of activation and inactivation, as well as V_{50} and slope of the voltage dependence of inactivation. If mutants for this locus become available, it will be interesting to see their effect upon the photoreceptor delayed rectifier currents.

There are also indications of a third, noninactivating potassium channel in the photoreceptors. The whole-cell outward current includes a ≈10% maintained component that is relatively resistant to block by quinidine and TEA. A candidate

channel for this conductance was encountered in just one cell-attached patch. The gating behavior (short openings, with voltage-dependent frequency) was similar to that of so-called K_o channels in *Drosophila* embryonic myotubes (Zagotta et al., 1988); however, the single-channel conductance (≈5–10 pS) was much smaller.

Functional considerations

Most neurons studied have a collection of distinct potassium channels (Rudy, 1988), although the functional roles of the different components are not always apparent. Any attempt at a serious analysis of function in previously available neuronal preparations from *Drosophila* is restricted because of the heterogeneous collection of unidentified cells each with its own cocktail of currents. By contrast, the present preparation represents an identified class of sensory neuron, whose function as a photoreceptor has been extensively studied by intracellular recordings in the intact retina, both in *Drosophila* and in even more detail in related Diptera such as *Calliphora* and *Musca* (reviews: Hardie, 1985; Selinger and Minke, 1988).

Invertebrate photoreceptors generate a maintained depolarization in response to light by activation of cation channels. The resulting activation of voltage-sensitive potassium channels will oppose this light-induced depolarization and can be predicted to sharpen transient responses and increase the dynamic range of the cell by preventing it from saturating in response to bright illumination. In addition, for a given depolarization a much lower resistance of the cell is allowed by the simultaneous activation of two antagonistic conductances. This has the consequence of reducing the membrane time constant and allowing the transmission of high-frequency signals that would otherwise be attenuated by the membrane time constant of the cell. In a recent study (Weckström et al., 1991), we have characterized what are possibly homologous potassium conductances in the blowfly, *Calliphora,* and presented direct evidence for these functional roles. The equivalent experiments in *Drosophila* have yet to be performed; however, a combination of mutant and pharmacological analysis clearly has the potential to address very directly the roles of these conductances in determining photoreceptor performance. From a comparison of the operating ranges of the conductances characterized in the present study, and the presumed operating range of the photoreceptor (≈ −60 to +10 mV), one can suggest that the slowly inactivating delayed rectifier current in combination with the maintained outward current may be well suited to play a similar role to the conductances we have characterized in *Calliphora.* It will be more of a challenge, however, to identify the roles of the rapidly inactivating conductances, I_A and I_{Kf}. Unless the *in situ* resting potential of photoreceptors (−50 to −60 mV) has been seriously underestimated, both these currents are likely to be completely inactivated except at very low light levels. In this respect, and bearing in mind the lability of I_{Kf} and the drift in voltage dependence of I_{Ks} (Fig. 10*b*), it will be worth addressing the question of whether any of the three conductances described may be subject to modulation. Possible candidate processes known or believed to exist in the arthropod retina include a rise in intracellular calcium during light adaptation (Levy and Fein, 1985), light-induced activation of protein kinase C (Minke et al., 1990), and possible modulation by efferent serotonergic fibers terminating near the photoreceptor axons in the first visual neuropil (Nässel, 1987).

Along with a parallel study of the same cells (Hardie et al., 1991), the present work introduces what is potentially a powerful new preparation for the combined biophysical and molecular investigation of ion channels. From a molecular biological point of view, the retina is probably already the most intensively investigated tissue in *Drosophila,* particularly with respect to development and phototransduction (reviews: Selinger and Minke, 1988; Ready, 1989). The possibility of patch-clamping these well-studied cells should provide many opportunities for studies of a variety of photoreceptor processes, in addition to the roles of voltage-sensitive conductances considered here.

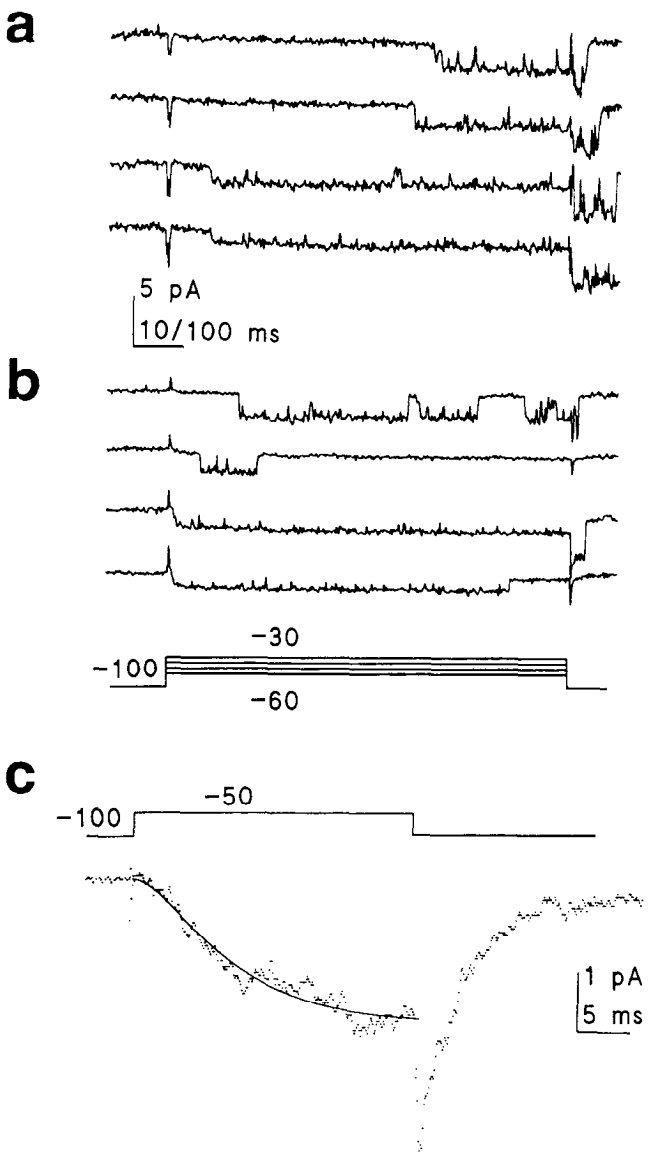

Figure 14. I_{Ks} channels. Single channels recorded in cell-attached patches from adult Sh^{KS133} photoreceptors with high (200 mM)-K patch pipettes (currents inward). *a,* Activation of a single presumptive I_{Ks} channel to voltage steps between −60 mV (*top trace*) and −30 mV (*bottom trace*), from a holding potential of −100 mV. Slope conductance determined by regression analysis was 30.5 pS. *b,* Same voltage protocol on a 10× longer time scale showing very long openings. *c,* Ensemble average for channel openings at −50 mV. The activation time course has been fit with a time constant of 6 msec (*solid curve,* assuming Eq. 2, $n = 2$). This is close to the activation time constant of I_{Ks} at −30 mV in whole-cell recordings (see Fig. 11).

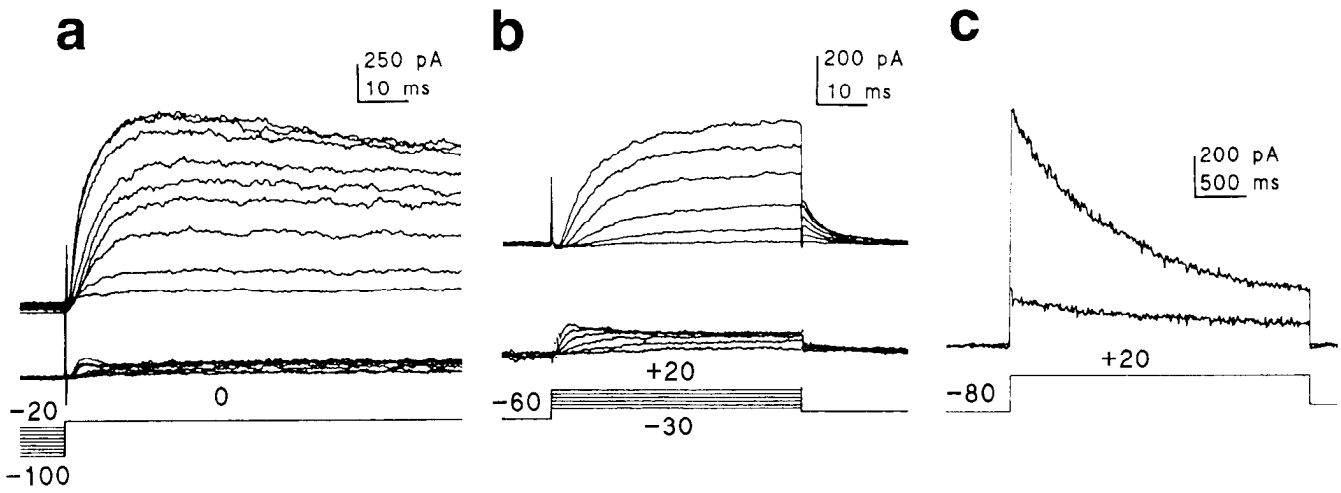

Figure 15. Effects of quinidine on potassium conductances. All panels show control responses (*upper traces*) with responses to identical voltage protocols in the presence of quinidine in the bath (*lower traces*). *a*, A photoreceptor showing all three components of potassium conductance, elicited following hyperpolarizing prepulses from −20 to −100 mV. Bath application of 100 μM quinidine reduces both $I_{K'}$ and I_{Ks} by at least 90%. However, a small I_A component is revealed that was previously masked by the much larger delayed rectifier currents. Recording is from a wild-type p11 photoreceptor—the stage at which I_A first becomes detectable. *b*, Quinidine block is voltage and/or state dependent. From a holding potential of −60 mV, only I_{Ks} is recruited in a p11 wild-type photoreceptor. During a partial quinidine block (after partial washout of 100 μM quinidine), the initial rising phases of the responses are little affected. However, increasingly at more depolarized voltages (−30 to +20 mV steps) a block develops rapidly resulting in responses that appear to inactivate above 0 mV. *c*, Quinidine has less effect on the maintained component: during a 100 μM quinidine block, the residual current shows significantly less inactivation than the control.

References

Bainbridge SP, Bownes M (1981) Staging the metamorphosis of *Drosophila melanogaster*. J Embryol Exp Morphol 66:57–80.

Baker K, Salkoff L (1990) The *Drosophila Shaker* gene codes for a distinctive K^+ current in a subset of neurons. Neuron 4:129–140.

Baumann A, Krah-Jentgens I, Müller R, Muller-Holtkamp F, Seidel R, Kecskemethy N, Casal J, Ferrus A, Pongs O (1987) Molecular organization of the maternal effect region of the *Shaker* complex of *Drosophila*: characterization of an I_A channel transcript with homology to vertebrate Na^+ channel. EMBO J 6:3419–3429.

Butler A, Wei A, Baker K, Salkoff L (1989) A family of putative K channel genes in *Drosophila*. Science 243:943–947.

Byerly L, Leung H-T (1988) Ionic currents of *Drosophila* neurons in embryonic cultures. J Neurosci 8:4379–4393.

Drysdale R, Warmke J, Kreber R, Ganetzky B (1991) Molecular characterization of *eag*: a gene affecting potassium channels in *Drosophila melanogaster*. Genetics 127:497–505.

Fenwick EM, Marty A, Neher E (1982a) A patch-clamp study of bovine chromaffin cells and their sensitivity to acetylcholine. J Physiol (Lond) 331:577–597.

Fenwick EM, Marty A, Neher E (1982b) Sodium and calcium channels in bovine chromaffin cells. J Physiol (Lond) 331:599–635.

Fernandez JM, Fox AP, Krasne S (1984) Membrane patches and whole-cell membranes: a comparison of electrical properties in rat clonal pituitary (GH3) cells. J Physiol (Lond) 356:565–585.

Ganetzky B, Wu C-F (1985) Genes and membrane excitability in *Drosophila*. Trends Neurosci 8:322–326.

Hamill OP, Marty A, Neher E, Sakmann B, Sigworth F (1981) Improved patch clamp techniques for high resolution current recording from cells and cell-free membrane patches. Pfluegers Arch 391:85–100.

Hardie RC (1985) Functional organization of the fly retina. Prog Sens Physiol 5:1–79.

Hardie RC (1989) A histamine-gated chloride channel involved in synaptic transmission at a photoreceptor synapse. Nature 339:704–706.

Hardie RC, Voss D, Pongs O, Laughlin SB (1991) Novel potassium channels encoded by the *Shaker* gene in *Drosophila* photoreceptors. Neuron 6:477–486.

Harris WA, Stark WS, Walker JA (1976) Genetic dissection of the photoreceptor system in the compound eye of *Drosophila melanogaster*. J Physiol (Lond) 256:415–439.

Hermann A, Gorman ALF (1984) Action of quinidine on ionic currents of molluscan pacemaker neurons. J Gen Physiol 83:919–940.

Hille B (1984) Ionic channels of excitable membranes. Sunderland, MA: Sinauer.

Isacoff EY, Jan YN, Jan LY (1990) Evidence for the formation of heteromultimeric potassium channels in *Xenopus* oocytes. Nature 345:530–534.

Iverson LE, Rudy B (1990) The role of divergent amino and carboxyl domains on the inactivation properties of potassium channels derived from the *Shaker* gene of *Drosophila*. J Neurosci 10:2903–2916.

Iverson LE, Tanouye MA, Lester HA, Davidson N, Rudy B (1988) A-type potassium channels expressed from *Shaker* locus cDNA. Proc Natl Acad Sci USA 85:5723–5727.

Johnson EC, Pak WL (1986) Electrophysiological study of *Drosophila* rhodopsin mutants. J Gen Physiol 88:651–673.

Kamb A, Iverson LE, Tanouye MA (1987) Molecular characterization of *Shaker*, a *Drosophila* gene that encodes a potassium channel. Cell 50:405–413.

Kamb A, Tseng-Crank J, Tanouye MA (1988) Multiple products of the *Drosophila Shaker* gene may contribute to potassium channel diversity. Neuron 1:421–430.

Levy S, Fein A (1985) Relationship between light sensitivity and intracellular free Ca concentration in *Limulus* photoreceptors. J Gen Physiol 85:805–841.

Lichtinghagen R, Stocker M, Wittka R, Boheim G, Stühmer W, Ferrus A, Pongs O (1990) Molecular basis of altered excitability in *Shaker* mutants of *Drosophila melanogaster*. EMBO J 9:4399–4407.

Marty A, Neher E (1983) Tight-seal whole-cell recording. In: Single-channel recording (Sakmann B, Neher E, eds), pp 107–122. New York: Plenum.

McCormack K, Lin JW, Iverson LE, Rudy B (1990) *Shaker* K^+ channel subunits form heteromultimeric channels with novel functional properties. Biochem Biophys Res Commun 171:1361–1371.

McKinnon R, Yellen G (1990) Mutations affecting TEA blockade and ion permeation in voltage-activated K^+ channels. Science 250:276–279.

Minke B, Rubinstein CT, Sahly I, Bar-Nachum S, Timberg R, Selinger Z (1990) Phorbol ester induces photoreceptor-specific degeneration in a *Drosophila* mutant. Proc Natl Acad Sci USA 87:113–117.

Nässel DR (1987) Serotonin and serotonin containing neurons in the nervous systems of insects. Prog Neurobiol 30:1–85.

Pak WL (1979) Study of photoreceptor function using *Drosophila* mutants. In: Neurogenetics: genetic approaches to the nervous system (Breakfield X, ed), pp 67–99. New York: Elsevier North-Holland.

Pak WL (1991) The molecular biology of the retina: basic and clinically relevant studies. Molecular genetic studies of photoreceptor function using *Drosophila* mutants. Prog Clin Biol Res 362:1–32.

Papazian DM, Schwarz TL, Tempel BL, Jan YN, Jan LY (1987) Cloning of genomic and complementary DNA from *Shaker*, a putative potassium channel gene from *Drosophila*. Science 237:749–753.

Papazian DM, Schwarz TL, Tempel BL, Timpe LC, Jan LY (1988) Ion channels in *Drosophila*. Annu Rev Physiol 50:379–394.

Pongs O, Kecskemethy N, Muller R, Krah-Jentgens I, Baumann A, Kiltz HH, Canal I, Llamazares S, Ferrus A (1988) *Shaker* encodes a family of putative potassium channel proteins in the nervous system of *Drosophila*. EMBO J 7:1087–1096.

Ready DF (1989) A multifaceted approach to neural development. Trends Neurosci 12:102–110.

Rudy B (1988) Diversity and ubiquity of K channels. Neuroscience 25:729–749.

Sakmann B, Neher E (1983) Geometric parameters of pipettes and membrane patches. In: Single-channel recording (Sakmann B, Neher E, eds), pp 37–51. New York: Plenum.

Salkoff L (1983) Genetic and voltage-clamp analysis of a *Drosophila* potassium channel. Cold Spring Harbor Symp Quant Biol 48:221–231.

Salkoff L, Tanouye MA (1986) Genetics of ion channels. Physiol Rev 66:301–329.

Salkoff L, Wyman RJ (1981a) Outward currents in developing *Drosophila* flight muscle. Science 212:461–463.

Salkoff L, Wyman RJ (1981b) Genetic modification of potassium channels in *Drosophila Shaker* mutants. Nature 293:228–230.

Salkoff L, Wyman RJ (1983) Ion currents in *Drosophila* flight muscles. J Physiol (Lond) 337:687–709.

Schwarz TL, Tempel BL, Papazian DM, Jan YN, Jan LY (1988) Multiple potassium-channel components are produced by alternative splicing at the *Shaker* locus in *Drosophila*. Nature 331:137–142.

Schwarz TL, Papazian DM, Carretto RC, Jan YN, Jan LY (1990) Immunological characterization of K^+ channel components from the *Shaker* locus and differential distribution of splicing variants in *Drosophila*. Neuron 4:119–127.

Selinger Z, Minke B (1988) Inositol lipid cascade of vision studied in mutant flies. Cold Spring Harbor Symp Quant Biol 53:333–341.

Singh S, Wu C-F (1989) Complete separation of four potassium currents in *Drosophila*. Neuron 2:1325–1329.

Solc CK, Aldrich RW (1988) Voltage-gated potassium channels in larval CNS neurons of *Drosophila*. J Neurosci 8:2256–2570.

Tanouye MA, Ferrus A, Fujita SC (1981) Abnormal action potentials associated with the *Shaker* complex locus of *Drosophila*. Proc Natl Acad Sci USA 78:6548–6552.

Tempel BL, Papazian DM, Schwarz TL, Jan YN, Jan LY (1987) Sequence of a probable potassium channel component encoded at *Shaker* locus of *Drosophila*. Science 237:770–775.

Timpe LC, Schwarz TL, Tempel BL, Papazian DM, Jan YN, Jan LY (1988) Expression of functional potassium channels from *Shaker* cDNA in *Xenopus* oocytes. Nature 331:143–145.

Weckström M, Hardie RC, Laughlin SB (1991) Voltage-activated potassium channels in blowfly photoreceptors and their role in light adaptation. J Physiol (Lond) 440:635–657.

Wei A, Covarrubias M, Butler A, Baker K, Pak M, Salkoff L (1990) K^+ current diversity is produced by an extended gene family conserved in *Drosophila* and mouse. Science 248:599–603.

Wu C-F, Haugland FN (1985) Voltage clamp analysis of membrane currents in larval muscle fibers of *Drosophila*: alteration of potassium currents in *Shaker* mutants. J Neurosci 5:2626–2640.

Wu C-F, Pak WL (1975) Quantal basis of photoreceptor spectral sensitivity of *Drosophila melanogaster*. J Gen Physiol 66:149–168.

Wu C-F, Ganetzky B, Haugland FN, Liu A-X (1983a) Potassium currents in *Drosophila*: different components affected by mutations of two genes. Science 220:1076–1078.

Wu C-F, Suzuki N, Poo M-M (1983b) Dissociated neurons from normal and mutant *Drosophila* larval central nervous system in cell culture. J Neurosci 3:1888–1899.

Yamamoto D, Suzuki N (1989) Characterization of single non-inactivating potassium channels in primary neuronal cultures of *Drosophila*. J Exp Biol 145:173–184.

Zagotta WN, Aldrich RW (1990) Voltage-dependent gating of *Shaker* A-type channels in *Drosophila* muscle. J Gen Physiol 95:29–60.

Zagotta WN, Brainard MS, Aldrich RW (1988) Single-channel analysis of four distinct classes of potassium channels in *Drosophila* muscle. J Neurosci 8:4765–4779.

Zagotta WN, Germeraad S, Garber SS, Hoshi T, Aldrich RW (1989) Properties of *ShB* A-type potassium channels expressed in *Shaker* mutant *Drosophila* by germline transformation. Neuron 3:773–782.